

Relate macroseismic intensity (EMS-98) to ground-motion parameters

Work Package 6 "Ground-motion for engineers"



AUTHORS		REVIEW		APPROVAL	
Name	Date	Name	Date	Name	Date
Marco Fasan	2019/09/30	Reviewers name and kawase	YYYY/MM/DD 2020/12/07	 Public-access SIGMA-2 restricted	YYYY/MM/DD

Document history

DATE	VERSION	COMMENTS
YYYY/MM/DD	0	

Executive summary

The actual practice of seismic-risk assessment for critical infrastructures is based on Uniform Hazard Spectra (UHS) derived from Probabilistic Seismic Hazard Assessment (PSHA) in the format of (pseudo) spectral accelerations. The spectral (force-based) method is still widely applied in earthquake engineering, especially in the design of systems. It is also applied in fragility analysis. The UHS and subsequently the time-history derived based on it has the problem that in reality it does not represent a uniform hazard but the weighted contribution of earthquakes leading to very different intensities at the plant site.

Macroseismic intensity represents a measure of the strength of an earthquake record inferred from observed damage. According to the European Macroseismic Scale (EMS), different earthquakes characterized by the same macroseismic intensity should lead to the same mean observed damage on buildings with homogenous characteristics (vulnerability classes). At the same time, macroseismic intensity allows to consider the variability on the ground motion parameters associated with the same level of damage. Therefore, to perform non-linear time-history analyses with intensity-consistent sets of accelerograms, means to subject the structures to the same damaging potential and to catch the variability on ground motion parameters.

In this work, relations between ground motion characteristics and EMS macroseismic intensity are investigated. These relations are based on chi-square analysis between intensity and linear or non-linear ground motion parameters.

The way macroseismic intensity is assigned on field is replicated numerically extracting non-linear demand parameters from non-linear time history analysis using non-linear SDOF systems representative of the non-linear behaviour of different buildings vulnerability classes.

A database of intensity (EMS) consistent natural accelerograms is developed starting from existing catalogues of records and observed intensity.

Table of Contents

Document history.....	2
Executive summary	2
Introduction	5
1. Short literature Review	6
2. Data collection	7
3. Proposed methodology.....	14
4. Results, comments and comparisons.....	20
5. Conclusions	31
Bibliography	32
APPENDIX 1 Performed tests	34
APPENDIX 2 Regression coefficients for the GMPs	37
APPENDIX 3 Description of the header of the final database flatfile	39
APPENDIX 4 Characteristics of the modelled SDOF systems.....	41



Introduction

Classical Performance Based Seismic Design (PBSD) and seismic-risk assessment is based on Probabilistic Seismic Hazard Assessment (PSHA) (Cornell 1968) using as representative ground motion intensity measure the spectral acceleration. This procedure leads to the definition of the Uniform Hazard Spectrum (UHS), that is, a response spectrum that shows at each vibrational period the spectral acceleration having a predefined probability of exceedance in a fixed period of time. UHS represents a weighted value due to the contribution of different earthquakes having different damaging potential (Klügel and Stäuble-Akçay 2018), this is illustrated in a qualitative manner in Figure 1. Therefore, if a UHS is used as target spectrum, even when selecting spectrum compatible accelerograms the final structural demands will be affected by the different damaging potential of each selected accelerogram, hence the structures under analysis are not subject to a uniform hazard. Moreover, even if spectral acceleration represents an efficient intensity measure, it still represents a peak and summary value and therefore cannot capture the damaging features of the earthquake that depends on the time evolution (incl. duration) of the accelerations.

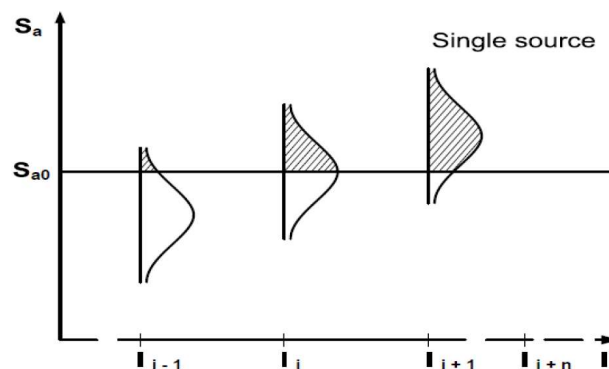


Figure 1: Illustration of the calculation concept of PSHA (example for a single source that with different frequency can cause earthquakes of different strength leading to different site intensities).

Seismic Hazard Assessment (either probabilistic or deterministic) can be done also using macroseismic intensity as intensity measure taking advantage of the longer duration of historical catalogues compared with instrumental ones. Differently from spectral acceleration, theoretically macroseismic intensity represents a measure of the strength of the ground shaking inferred from the mean damage observed in a homogeneous area. In other words, buildings are used as sensors and the extent of damage is used as a measure of the strength of the signal. In particular, the European Macroseismic Scale - EMS (Grünthal 1998) should lead to consistent measures of the strength of the signal even if the built environment where the macroseismic intensity is assessed is very different. In other words, if the same earthquake (the same recorded signal) happens in two different cities with two different built environments, the evaluation of the intensity using the EMS should lead to the same value. This is assured subdividing buildings in different vulnerability classes and observed damage in different damage grades. Clearly, each step performed in the assignment of intensity introduce new uncertainties on the real intensity value. Uncertainties are mainly related to the subjectivity on the field definition of (Musson et al. 2010):

- Vulnerability class of the building;
- Damage grade reached by the building.

Since macroseismic intensity is directly based on observed damage, it follows that accelerograms having the same macroseismic intensity show the same damaging potential. Based on this consideration, non-linear time history analysis performed with accelerograms having the same macroseismic intensity should lead to a damage consistent evaluation of the performance of a building (or a stock of buildings), therefore to a damage-consistent risk analysis.

Actually, linking a macroseismic intensity with a single accelerogram introduces new uncertainties due to the spatial variability of the ground motion. In fact, since macroseismic intensity is defined over an area it would be more correct to assign it to a wave field and not to a single record.

In this work a methodology to assign the EMS macroseismic intensity (I_{EMS}) to accelerograms is proposed using regression analysis on available data. In fact, few accelerograms are recorded directly inside areas where the macroseismic intensity is evaluated too. Hence, the possibility to assign the intensity to a recorded or simulated accelerogram can help to perform damage consistent risk assessments, increasing the number of available accelerograms to be used.

The EMS is chosen since it is the reference macroseismic scale in Europe since 1998 and its vulnerability model is the most complete and updated. Nevertheless, the same procedure proposed here can be applied with any macroseismic scale.

Many authors proposed regression equations between ground motion parameters and macroseismic intensity but few are developed for EMS and none of them tried to replicate numerically the way EMS is assigned in the field.

The proposed methodology tries to simulate numerically the assignment procedure of macroseismic intensities on field and is based on regression equations between intensity and linear or non-linear ground motion parameters. Non-linear parameters are extracted from non-linear time history analysis using non-linear SDOF systems representative of the non-linear behaviour of different buildings vulnerability classes.

The methodology, is developed and proposed in the framework of the European project Seismic Ground Motion Assessment 2 (SIGMA-2, <http://www.sigma-2.net/>).

The final purpose is to create a database of damage-consistent natural and synthetic accelerograms to be used to perform intensity-based fragility assessment and subsequent seismic risk analysis.

1. Short literature Review

Many authors proposed regression equations between ground motion parameters and macroseismic intensity. Generally, a linear relation is proposed between the macroseismic intensity and the logarithm of some ground motion parameters (GMPs), mainly using peak values such as PGA, PGV and PGD as independent variables. The variability among of the proposed correlations is related to the use of different datasets and different macroseismic intensity scales such as the Mercalli-Cancani-Sieberg (MCS), the Modified Mercalli (MM), or the Medvedev-Sponheuer-Karnik (MSK) scales.

Concentrating on the most recent works, Gomez Capera et al. (2007) proposed a relation between PGA and MCS intensity recorded in Italy, using Orthogonal Distance Regression (ODR) that allows to take into account uncertainties on both independent and dependent variable. Tselentis and Danciu (2008) proposed relations between MMI-GMPs valid for Greece using a dataset of 310 time histories recorded from 89 Greek earthquakes. The general criterion was to allocate at each station the nearest MMI values within an uncertainty of one unit to every station. Weighted linear regression was used as fitting techniques and found that the lowest standard deviation for the predictive model was for PGA. Weight assigned to each MMI level was based on the number of observations. Statistical significance of each regression coefficient was tested using the t-test. The significance of including the magnitude in the regression models was also tested and results show that the magnitude was significant only in the case of MMI predicted from PGA. Faenza and Michelini (2010, 2011) extracted, for the Italian territory, all the localities reporting MCS intensity data located within 3 km from recorded accelerograms and associated the closest Macro Data Point (MDP) to the recorded GMP. Their database consists of 66 Italian earthquakes which occurred in the time span 1972–2004 ($3.9 \leq M_w \leq 6.9$) and intensity $MCS \leq 8$ for a total of 266 pairs Intensity-GMP. They used ODR but grouped the peak values in intensity classes at 0.5 intensity intervals and perform the regression on the mean values using the corresponding standard

deviations. The intensity standard deviations have been set equal to 0.5. Bilal and Askan (Bilal and Askan 2014) proposed relations between MM intensity and GMPs using observations recorded in Turkey. A mean GMP is assigned to each macroseismic intensity level and multivariate linear regression analyses is adopted. The functional form included the magnitude M_w and the epicentral distance R_{epi} and variations of residuals show that these two parameters do not add better information than the GMP alone. It is also observed that relationships should be derived from regional datasets because both the ground-motion content and damage types exhibit local properties. The regional dependency of macroseismic intensity was also confirmed by Caprio et al. (2015). Gomez Capera et al. (2015) developed a dataset valid for the Italian territory that consists of 118 pairs of MDP-GMP from 53 earthquakes in time span 1976-2009 and ranging between $3-4 \leq MCS \leq 8-9$ for the macroseismic intensity and ranging between $3.9 \leq M_w \leq 6.9$ for the momentum magnitude. GMP is defined as the largest of the horizontal components (max component) and the maximum distance between macroseismic observations and ground-motion station that recorded the data is 6 km. For each macroseismic intensity level, the mean and the standard deviation with respect to the mean value of the selected ground-motion parameters are computed and ODR is performed on mean values instead of using single data pairs. The work of Zanini et al. (2019) is the first one where relations intensity - GMPs are developed using the European Macroseismic Scale (EMS) as reference. The final dataset consists of 220 data pairs from 22 earthquakes which occurred in the time span between 1983 and 2016 ($3.2 \leq M_w \leq 6.1$), with $I_{EMS} \leq 10$. The association of macroseismic intensity with GMPs was carried out for the sites located within 3 km from an accelerometric station, pairing each intensity point with the closest station. The regression analysis follows the methodology proposed by Faenza et al. (2010). Relations were compared with those proposed for other intensity scales and the slope of the proposed regressions was found lower than the ones of most of other equations. Masi et al. (2020) operates similarly to Zanini et al. (2019) but proposed bi-linear regressions using both MCS and EMS intensity.

Literature on macroseismic intensity highlight how the huge variability on observed GMPs and intensity values is linked with a different spatial representativeness of the two measures. GMPs are punctual measures valid only in the vicinity of the recorded station whereas the macroseismic intensity is an integral measure defined over an area and over the damage occurred on buildings with different vulnerabilities. It is important to note how the influence of seismic sequences or the maximum distance between the macrodata point and the recording station was never accounted for in proposed correlations. Many field surveys are carried after more than one damaging earthquake occurs and therefore the observed intensity, even if very close to the recording station, represents a “cumulative” macroseismic intensity. Every time there is a seismic sequence, even if the survey is carried out soon after every damaging earthquake occurs, the observed intensity has to be intended as a cumulative value as also evidenced by Graziani et al. (2019). A first simplified methodology to assess the influence of cumulative damage due seismic sequences on macroseismic intensity was proposed by Grimaz and Malisan (2017).

To avoid the large scatter of the peak ground motion data for each intensity unit, many papers use averages of data grouped into intensity classes. However, correlations based on averages can be misleading since different intensities classes are not equally represented and there are not enough data for some intensity classes to establish averages and standard deviations.

2. Data collection

The procedure proposed to assemble the combined database of records and observed Macroseismic Intensity consists in downloading the macrodata points (MDP) and the natural records from available databases and linking them using a maximum distance between the MDP and the record station. Similar procedures have been followed by many authors in order to develop linear regressions between macroseismic intensity and ground motion parameters, see for example Bilal and Askan (Bilal and

Askan 2014), Faenza and Michelini (2010, 2011), Gomez Capera et al. (2007, 2015), Zanini et al. (2019), Masi et al. (2020).

The MDPs have been gathered mainly from the 2015 version of the Italian Macroseismic Database (DBMI) (Locati et al. 2016). The recorded accelerograms have been downloaded from the European Strong Motion Database (ESM) (Lanzano et al. 2019). ESM database allows downloading records of events having magnitude $M \geq 4$, mainly recorded in the European-Mediterranean and the middle-East regions. The accelerograms to be downloaded were identified starting from the event date and time reported in the CPTI catalogue and looking for them inside the ESM flatfile (Lanzano et al. 2019)

DBMI is updated to 2015 and assembled mainly in MCS scale (Mercalli-Cancani-Sieberg), however for many events the EMS intensity is also available. For the purpose of this study only I_{EMS} MDPs have been retained. Data have also been integrated with publications available in literature in order to account for events happened after 2015 and for past events where the macroseismic intensity was reevaluated using EMS scale. The following data have been used to integrate the MDPs available in DBMI:

- data of the 6 May 1976 Friuli earthquake were replaced with those available in Tertulliani et al. (2018) that re-evaluated the macroseismic intensity using the EMS and available surveys;
- data on MCS intensity of the 7 and 11 May 1984 central Italy earthquakes were replaced with those available in Graziani et al. (2017) defined in EMS intensity;
- replacing data of the 14 September 2003 Appennino Bolognese earthquake bases on information provided by the QUEST group (Quick Earthquake Survey Team);
- replacing data of the 6 April 2009 L'Aquila earthquake with those available in Azzaro et al. (2011);
- adding data of the 25 January 2012 Emilia earthquake available in Tertulliani et al. (2012);
- replacing data of the 21 June 2013 Lunigiana earthquake based on information provided by QUEST;
- adding data of the 2016 Central Italy earthquake sequence available in Arcoraci et al. (2019).

Initially a total number of 143 common events were found cross-matching DBMI with the ESM database. The time span is 1972 – 2016 (respectively the year of the first Italian accelerogram in ESM and the year of the last observed macroseismic data point in the gathered documents). These 143 events correspond to 2412 records in ESM and 32862 MDPs. The moment magnitude M_w ranges from the 3.9 of the 15/12/2005 Val Nerina earthquake to the 6.9 of the 23/11/1980 Irpinia earthquake whereas the macroseismic intensity ranges $II \leq I_{EMS} \leq XI$. In particular, 8563 MDPs are evaluated in EMS scale (corresponding to 37 events).

In DBMI and other references, MDPs are reported with non-conventional intensities (using letters instead of roman or Arabian numbers) when available data are not enough to assign a proper intensity, that is when it is not possible to make reliable statistics on observed damage. These MDPs have not been considered in data processing since they are not representative of a proper macroseismic intensity. Regarding the records, only accelerograms that can be considered registered on free field have been retained, excluding those recorded in non-conventional locations such as buildings floors or balconies.

To link the MDPs with the records a criterion must be adopted. In literature, the link is established based on the distance between the MDP and the record station. Usually a maximum distance ranging between 6 km to 3 km is used. This is justified since it could represent the average length of a village to which the intensity is assigned (since macroseismic intensity is an average measure over an area).

As exposed in section 3 the effect of different maximum distances was investigated and, up to 3 km, did not affect the much the results. For this reason, in this study the final maximum distance is set equal to 3 km. After limiting the distance MDP-Station to 3 km and removing the non-conventional values the total number of couples MDP-GMP included in the initial database are 445 deriving from 228 records of 32 different earthquakes. Table 1 shows the data of the events included in the initial database. In

particular it includes the event ID reported in the ESM database, along with event date, latitude, longitude, depth, moment magnitude (M_W) and local magnitude (M_L). The last column shows the number of couples MDP-record available from each event. The event with the highest number of MDPs is the 30/10/2016 Norcia earthquake with a moment magnitude $M_w=6.5$. Figure 2 shows the Magnitude vs Epicentral distance distribution of the records included in the initial dataset. Figure 3 shows the location of the events whereas Figure 4 shows the location of the couples MDP-record along with their observed intensity.

Table 1: Characteristics of the initial database

ID	Date	Lat	Lon	Depth	MW	ML	N° I-MDP
IT-1976-0002	06/05/1976	46.26	13.3	5.7	6.4	6.4	6
IT-1983-0004	20/07/1983	37.55	15.17	24.7	4.5	4.3	6
IT-1984-0004	07/05/1984	41.7	13.86	20.5	5.9	5.9	13
IT-1999-0012	14/02/1999	38.18	15.02	12	4.7	3.9	3
IT-2001-0008	22/04/2001	37.7	15.02	5	4.2	3.2	1
IT-2002-0007	05/04/2002	38.35	15.1	5	4.4	4.2	1
IT-2002-0024	06/09/2002	38.38	13.7	5	5.8	5.6	3
IT-2002-0040	27/10/2002	37.76	15.12	5	4.9	4.8	1
IT-2003-0048	14/09/2003	44.26	11.38	8.3	5.3	5	2
IT-2006-0059	27/02/2006	38.16	15.2	9.2	4.4	4.1	7
IT-2006-0302	19/12/2006	37.78	14.91	23.8	4.2	4.1	2
IT-2009-0009	06/04/2009	42.34	13.38	8.3	6.1	5.9	20
IT-2009-0317	08/11/2009	37.85	14.56	7.6	4.4	4.4	1
IT-2009-0323	15/12/2009	43.01	12.27	8.8	4.2	4.3	1
IT-2009-0328	19/12/2009	37.78	14.97	26.9	/	4.4	7
ISIDe-2166809	02/04/2010	37.8	15.08	0.3	/	4.3	1
IT-2010-0032	16/08/2010	38.35	14.89	13.5	4.7	4.8	3
EMSC-20110506_0000042	06/05/2011	37.8	14.94	20.4	4.3	4	1
IT-2011-0110	23/06/2011	38.06	14.78	7.3	4.5	4.4	7
IT-2011-0020	17/07/2011	45.01	11.37	2.4	4.8	4.8	4
IT-2011-0022	25/07/2011	45.02	7.37	11	4.3	4.3	4
IT-2012-0002	25/01/2012	44.87	10.51	29	5	5	3
IT-2012-0008	20/05/2012	44.9	11.26	9.5	6.1	5.9	1
IT-2012-0011	29/05/2012	44.84	11.07	8.1	6	5.8	35
IT-2012-0061	25/10/2012	39.87	16.02	9.7	/	5	15
IT-2013-0001	04/01/2013	37.88	14.72	9.6	4.3	4.4	2
IT-2013-0005	21/06/2013	44.13	10.14	7	5.1	5.2	8
IT-2013-0013	15/08/2013	38.11	14.91	19.4	/	4.5	6
EMSC-20160824_0000006	24/08/2016	42.7	13.23	8.1	6	6	36
EMSC-20161026_0000095	26/10/2016	42.91	13.13	7.5	5.9	5.9	22
EMSC-20161030_0000029	30/10/2016	42.83	13.11	9.2	6.5	6.1	222

Figure 5 shows the distribution of couples for each intensity degree arranged in bins with half degree width. The number of observations are almost evenly distributed among all the intensity classes with the exception of the degrees with $I_{EMS} \geq 10$. The choice of using half degrees has been done since macroseismic intensity is often reported using half degrees. However, since EMS scale defines only twelve degrees, the arrangement in bins with one degree width has also been analysed but has shown no influence on final results. Figure 6 shows that the distribution of the distances between the MDPs and the station that recorded the associated accelerogram is also constant whereas Figure 7 shows that the distribution of magnitudes among the observed MDPs is almost constant with the exception of MDPs associated with magnitudes higher than 6. This is mainly due to the high number of observations gathered for the Norcia earthquake.

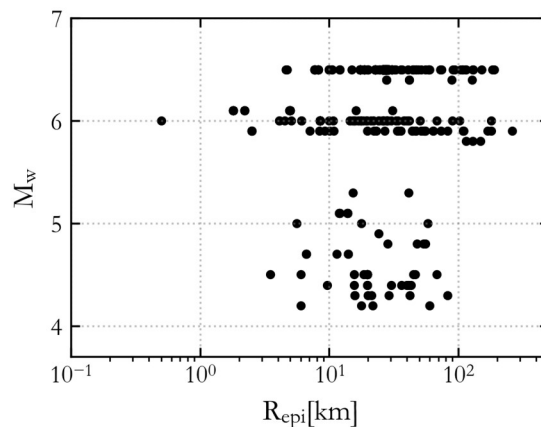


Figure 2: Magnitude vs Epicentral distance of the records included in the initial dataset.

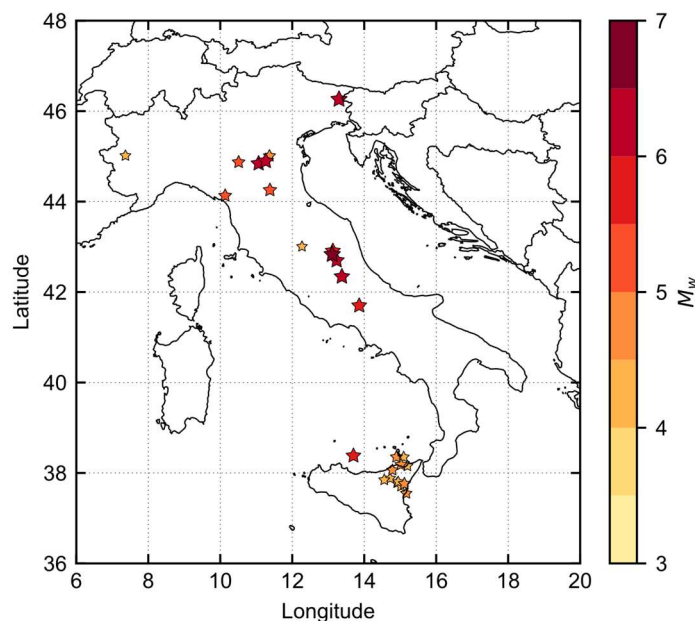


Figure 3: Location and magnitudes of the events included in the initial dataset.

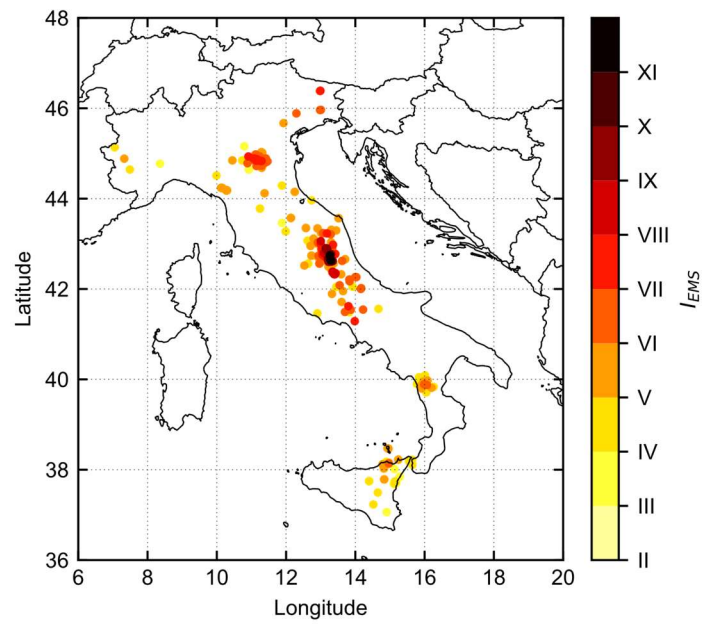


Figure 4: location of the MDPs included in the initial dataset along with macroseismic intensity

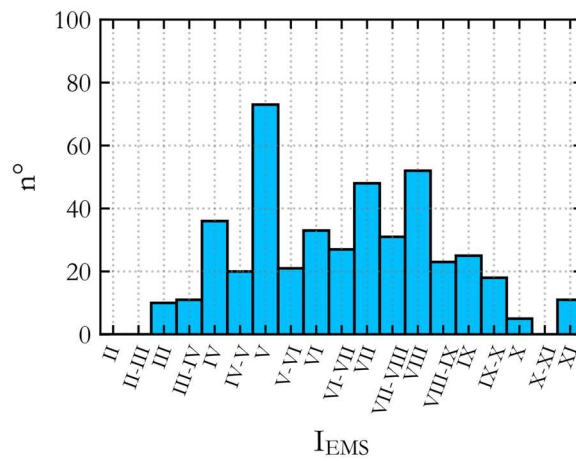


Figure 5: Distribution of couples MDP-record for each intensity degree.

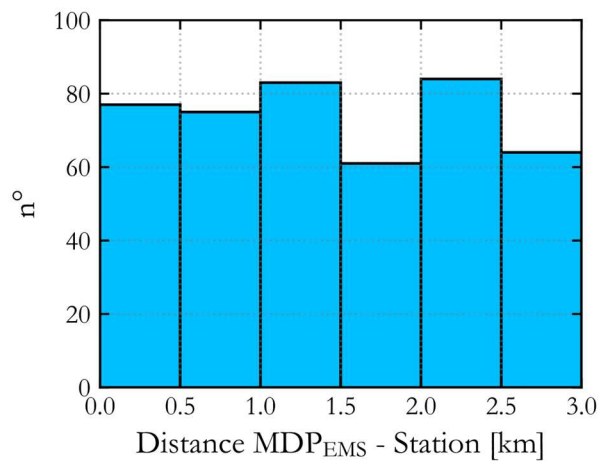


Figure 6: Distribution of the distance MDP-station of the recorded the accelerogram.

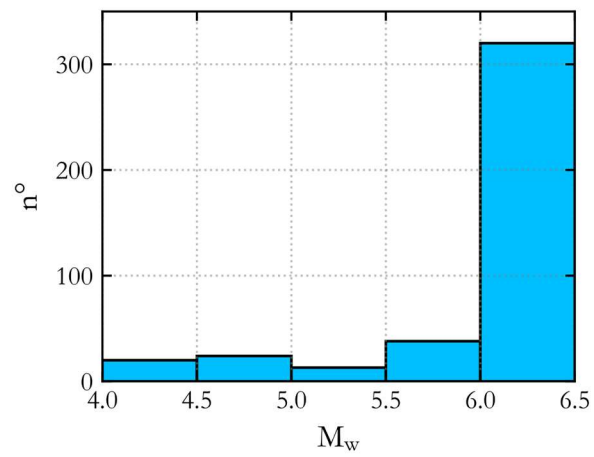


Figure 7: Distribution of couples MDP-record for different magnitude ranges present in the initial dataset

3. Proposed methodology

The main scope is to find the local relation between GMPs and macroseismic intensity defined according to the EMS scale. Many papers proposed regressions mainly in MCS or Modified Mercalli Intensity (MMI) using Ordinary Least Square (OLS) or Orthogonal Distance Regression (ODR). Up to now, the only regressions proposed in EMS intensity are published by Zanini et al. (2019) and Masi et al. (2020), allowing to establish EMS intensity from Peak Ground Acceleration (PGA), Velocity (PGV), Displacement (PGD), Housner and Arias Intensity.

In this report, linear chi-square regression (CSQ, a generalization of ODR) has been implemented since it allows to create invertible regressions that accounts for uncertainties in both variables (Lolli and Gasperini 2012). To perform CSQ it is necessary to know the standard deviations of both variables in order to correct the residuals around the fitting line (to calculate a standardized residual). In literature, this was often performed on averages of GMPs per intensity classes and the standard deviation assumed as the standard deviation of the averages. The intensity standard deviation was instead assumed equal to 0.5 (Faenza and Michelini 2010; Zanini et al. 2019). This choice reduce the scatter around the fitting line. At the same time, it can overestimate the real relation between the dependent and independent variable if the equation is used to infer conclusions about single observations (instead of mean of observations) since different intensities classes are not equally represented and there are not enough data for some intensity classes to establish averages and standard deviations (see APPENDIX 1). Looking at single observations scatter of data is huge due to the variation of ground motion parameters and includes at least:

- the variation $V_{GMP/EMS}$ of the GMPs given a macroseismic intensity occurred in an area;
- the variation $V_{EMS/GMP}$ of the response of the buildings once subjected to the one GMP.

In order to estimate the standard deviation σ_I of the intensity and σ_{IM} of the ground motion parameters (intensity measures), and to perform a correct CSQ, the following procedure have been adopted:

Objective: find the local relation between macroseismic intensity I_{EMS} and different ground motion parameters IM (e.g. PGA, PGV, PGD etc.);

Initial data: the initial data is the dataset presented in section 2 that represents the space distribution of observed intensity I in different localities and registered ground motion characteristic IM at different stations. In this dataset the average area, where the macroseismic intensity is assessed, is assumed to be a circle with 3 km radius;

Step 1: Identify the local space variability of I given IM (case a) and IM given I (case b) inside the circles of radius $R=3$ km.

- Case a)
 - for each event and recording station i , the variability is assessed using the range of the observed intensity I_{ij} inside a radius of 3 km centred on i :

$$V_i(I) = \max I_{i,j} - \min I_{i,j}$$

$V_i(I)$ is plotted against the natural logarithm of the number of intensities observed inside each circles centred on i station. Note that I_{ij} can also be represented by a logarithmic transformation (e.g $\ln(I_{i,j})$ or $\log(I_{i,j})$) depending on the chosen functional form of the regression.

- Case b)
 - for each event and place i with available macroseismic intensity, the variability is assessed using the range of the observed ground motion characteristic of interest IM_{ij} inside a radius of 3 km centred on i :

$$V_i(IM) = \max IM_{i,j} - \min IM_{i,j}$$

$V_i(IM)$ is plotted against the natural logarithm of the number of the ground motion characteristic of interest IM recorded inside each circles centred on i place.

Note that IM can also be represented by a logarithmic transformation of the ground motion parameters (e.g $\ln(\rho ga)$ or $\log(\rho ga)$) depending on the chosen functional form of the regression.

Step 2: Identify acceptable model distributions for the local data.

To judge about the statistical properties of the local data I and IM note the following: suppose we have a large sample of n independent random variables (ξ_1, \dots, ξ_n) with a cumulative distribution function $F(\xi)$ (in our case ξ is the local data of intensity I or ground motion parameter IM respectively). Then, the known extreme variables $\max \xi$ and $\min \xi$ should satisfy, in average, the following relations:

	$F(\max \xi_i) = 1 - \frac{1}{n}; \quad F(\min \xi_i) = \frac{1}{n}$	(1)
--	--	-----

Knowing the distribution $F(\xi)$, we can obtain the dependence of the sample range on sample volume, i.e.:

	$V_\xi = \max \xi - \min \xi \text{ vs } n$	
--	---	--

We can then compare the empirical relations produced at step 1 with theoretical ones. It allows to exclude obviously unacceptable models for the description of empirical data and to judge a reasonable standard deviation. Three theoretical models are used for comparison:

- $F(\xi)$ is a uniform distribution: i.e. the distribution density $f(\xi) = dF(\xi)dx$ is a constant in the interval $(0, V)$. In this case:

	$V_\xi(n) = V \left(1 - \frac{2}{n}\right) \approx V = \sigma_\xi \sqrt{12}$	(2)
--	--	-----

σ_ξ is the standard deviation of ξ . Indeed, the average of ξ in the considered interval is $V/2$ and the variation:

	$\sigma_\xi^2 = \int_0^V \left(\xi - \frac{V}{2}\right)^2 d\xi / V = \frac{V^2}{12}$	(3)
--	--	-----

- $F(\xi)$ is an exponential distribution $F(\xi) = 1 - \exp(-\frac{\xi}{\sigma_\xi})$, then by (1):

	$V_\xi(n) = \sigma_\xi \ln(n - 1)$	(4)
--	------------------------------------	-----

- If ξ has a Gaussian distribution, i.e. $f(\xi) = \exp(-\frac{\xi^2}{2\sigma_\xi^2})/\sqrt{2\pi\sigma_\xi^2}$, then by (1):

	$V_\xi(n) = \sigma_\xi \sqrt{8 \ln(n/\sqrt{2\pi})}$	(5)
--	---	-----

The similarity of theoretical and empirical distributions means the admissibility (consistency) of the theoretical models.

Step 3: Build a one-to-one dataset.

Having identified reasonable standard deviations, we need a one-to-one relation between I and GMP. A subset is created from the initial dataset matching the stations with the closest macrodata point. If a MDP is associated with two stations, only the pair with the shortest distance is retained. This is because the variation of this data pair inside the 3 km radius have already been assessed through the standard deviation of the two variables.

Step 4: Assuming the power law relation $I = aIM^b$, a chi-squared regression (CSQ) can be performed in the bi-logarithmic space using the linear functional form $\ln(I) = a + b\ln(IM)$ where a is the intercept of the regression line, b the slope and IM some ground motion parameter:

at this step the parameters a and b of the regression line are found minimizing the sum of the residuals R_i , using the following expression (CSQ):

	$\min \sum_{i=1}^N \frac{(\ln(I_i) - a - b\ln(IM_i))^2}{\sigma_{\ln(I)}^2 + b^2\sigma_{\ln(IM)}^2} = \chi^2$	(6)
--	--	-----

For large N and correct values of $\sigma_{\ln(I)}$ and $\sigma_{\ln(IM)}$, χ^2 has approximately a Normal distribution with mean N and standard deviation $\sqrt{2N}$. In fact, the square of a standard Gaussian variable has an average of 1 and a variance of 2. For the Central Limit theorem the sum of N of such independent variables has an average value of N and a variance of $2N$. Therefore, to test if the choice of the model parameters $\sigma_{\ln(I)}$ and $\sigma_{\ln(IM)}$ are consistent, this sum of the square of the standardized residuals χ^2 should satisfy the relation:

	$N - 3\sqrt{2N} \leq \chi^2 \leq N + 3\sqrt{2N}$	(7)
--	--	-----

Step 5: Identification of abnormal values of residuals R_i .

- abnormal residuals can be identified as those having a value higher than 3.

	$R_i = \frac{ \ln(I_i) - a - b\ln(IM_i) }{\sqrt{\sigma_{\ln(I)}^2 + b^2\sigma_{\ln(IM)}^2}} \geq 3$	(8)
--	---	-----

Step 6: Interpretation of abnormal values of residuals R_i and reduction of the dataset based on the this interpretation

Step 7: Repeat steps until all the criteria are met on average.

The proposed procedure is the outcome of several tests (the most meaningful are reported in APPENDIX 1), the first of which involved studying the relationship between the parameters as proposed by previous studies (binning the data in intensity classes, evaluate the standard deviation of the average values for each intensity class, perform orthogonal regression of the mean values). Some results of this preliminary tests are shown in Fasan et al. (2019) and do not show a good fit with the regression line. Moreover, the correlations based on averages can be misleading if they are used to make estimates on individual values because they overlook the variability across them assuming higher correlations than in reality. For these reasons, the proposed approach was preferred.

It is important to remind that macroseismic intensity is a measure of the strength of the signal inferred from observed mean damage. The main purpose on this study is to find the relation between the macroseismic intensity and the accelerogram that caused that macroseismic intensity. A recorded accelerogram represent a complete information of the ground motion at a specific point (site) and includes all the waveform modifications due to:

- local soil conditions;
- path effects, i.e. influence of the properties of soils crossed by waves from the source to the recording site;
- source effects due to the released energy and rupture process.

Since the accelerogram contains all these information, the investigated parameters in the regression analysis are only those extracted directly from the recorded ground motions. Therefore, information like soil type, epicentral distance, magnitude etc. were not included in the functional form of the regression. However, these kind of information are included in the final database. A description of the header of the final database reporting all the retained parameters is given in APPENDIX 3.

To the purpose of this study, 28 parameters have been used as independent GMPs. These have been divided in:

- non-structure specific intensity measures (Table 2);
- structure specific intensity measures derived from the response of linear SDOF (Table 3);
- structure specific intensity measures derived from the response non-linear SDOF systems (Table 4).

Moreover, all the regressions have been developed using the maximum horizontal component (*Max*) or the resultant of the two (*Res*, aka *MaxRotD100*).

The final scope is to assign a macroseismic intensity in order to separate accelerograms in damage consistent bins. Regressions based on average non-linear Engineering Demand Parameters (EDPs) should assure this consistency. In fact, EMS intensity represents an integral measure of the mean damage observed in a built environment. The EMS scale allows to assign intensity based on different grades of damage occurring in buildings of different vulnerability classes. The way EMS is assigned on field can be simulated numerically using non-linear time-history analysis (NLTHA) and modelling the behaviour of buildings of different vulnerability classes. To do so, in this study the different building typology and vulnerability classes included in the EMS have been modelled using 141 equivalent non-linear SDOF systems leading to a total initial number of 64296 NLTHAs (228 records, two components, 141 different SDOFs). The characteristics of these SDOFs (yielding force F_y , displacement δ_y and ductility μ) are extracted from Lagomarsino and Giovinazzi (2006) who proposed these values to develop a mechanical damage model in the framework of the RISK-EU project (Mouroux and Brun 2006) and are reported in APPENDIX 4 from Table 8 to Table 12. A bilinear non-degrading backbone with peak-oriented reloading stiffness was adopted as hysteretic behaviour. SDOF were modelled on OpenSEES using the modified peak oriented Ibarra-Medina-Krawinkler (IMK) hysteretic model (Ibarra et al. 2005). This hysteretic rule is able to account for the elongation of the structural period during a seismic event due to damage accumulation and it is therefore suited for the purposes of this study.

Table 2: Non structure-specific intensity measures.

Peak ground acceleration	$PGA = \max a_g(t) $	
Peak ground velocity	$PGV = \max v_g(t) $	
Peak ground displacement	$PGD = \max d_g(t) $	
Root-Mean-Square acceleration	$a_{RMS} = \sqrt{\frac{1}{t_{tot}} \int_{t_{tot}}^{t_{tot}} a_g(t)^2 dt}$	
Root-Mean-Square velocity	$v_{RMS} = \sqrt{\frac{1}{t_{tot}} \int_{t_{tot}}^{t_{tot}} v_g(t)^2 dt}$	
Root-Mean-Square displacement	$d_{RMS} = \sqrt{\frac{1}{t_{tot}} \int_{t_{tot}}^{t_{tot}} d_g(t)^2 dt}$	
Arias intensity	$AI = \frac{\pi}{2g} \int_0^{t_{tot}} a_g(t)^2 dt$	
Characteristic Intensity	$I_c = (a_{RMS})^{\frac{3}{2}} \cdot \sqrt{t_{tot}}$	(Park et al. 1985)
Cumulative Absolute Velocity	$CAV = \int_0^{t_{tot}} a_g(t) dt$	(Reed and Kassawara 1990)
Cumulative Absolute Displacement	$CAD = \int_0^{t_{tot}} v_g(t) dt$	
Specific Energy Density	$SED = \int_0^{t_{tot}} v_g(t)^2 dt$	
Maximum Incremental Velocity	$MIV = \max \left \int_{t_{(a_g(i)=0)}}^{t_{(a_g(i+1)=0)}} a_g(t) dt \right $	(Anderson and Bertero 1987)
Maximum Incremental Displacement	$MID = \max \left \int_{t_{(v_g(i)=0)}}^{t_{(v_g(i+1)=0)}} v_g(t) dt \right $	(Anderson and Bertero 1987)

a_g represents the record acceleration
 v_g represents the record velocity
 d_g represents the record displacement

Table 3: Structure-specific intensity measures – elastic.

Acceleration Spectrum Intensity	$ASI = \int_{0.1}^{0.5} PS_a(\xi = 0.05, T) dT$
Modified ASI – 1	$MASI_{0.1}^1 = \int_{0.1}^1 PS_a(\xi = 0.05, T) dT$
Modified ASI – 1.5	$MASI_{0.1}^{1.5} = \int_{0.1}^{1.5} PS_a(\xi = 0.05, T) dT$
Velocity Spectrum Intensity	$VSI = \int_{0.1}^{2.5} S_v(\xi = 0.05, T) dT$
Modified VSI – 1	$MVSI_{0.1}^1 = \int_{0.1}^1 S_v(\xi = 0.05, T) dT$
Modified VSI – 1.5	$MVSI_{0.1}^{1.5} = \int_{0.1}^{1.5} S_v(\xi = 0.05, T) dT$
Housner Intensity	$HI = \int_{0.1}^{2.5} PS_v(\xi = 0.05, T) dT$
Modified HI – 1	$MHI_{0.1}^1 = \int_{0.1}^1 PS_v(\xi = 0.05, T) dT$
Modified HI – 1.5	$MHI_{0.1}^{1.5} = \int_{0.1}^{1.5} PS_v(\xi = 0.05, T) dT$
Input Energy Spectral Intensity	$IESI_{0.1}^{0.5} = \int_{0.1}^{0.5} I_E(\xi = 0.05, T) dT$
Modified IESI – 1	$IESI_{0.1}^1 = \int_{0.1}^1 I_E(\xi = 0.05, T) dT$
Modified IESI – 1.5	$IESI_{0.1}^{1.5} = \int_{0.1}^{1.5} I_E(\xi = 0.05, T) dT$

PS_a is the pseudo spectral acceleration

PS_v is the pseudo spectral velocity

S_v is the spectral velocity

$I_E = -m \int_0^{t_{tot}} a_g(t) \cdot v(t) dt$ represents the input energy.

Table 4: Structure-specific intensity measures – inelastic.

Average kinematic ductility	$\mu_{kin,avg} = \frac{\sum_{i=1}^N \delta_{max,i}}{N \delta_{y,i}}$
Average cyclic ductility	$\mu_{cyc,avg} = \frac{\sum_{i=1}^N \frac{-\delta_{min,i} + \delta_{max,i}}{\delta_{y,i}}}{N}$
Average hysteretic ductility	$\mu_{H,avg} = \frac{\sum_{i=1}^N \frac{E_{H,i}}{F_{y,i} \delta_{y,i}} + 1}{N}$

$N = 141$ represents the number of SDOF systems used to describe the EMS building typologies.

$\delta_{max,i}$ is the maximum displacement reached by SDOF i

$\delta_{min,i}$ is the minimum displacement reached by SDOF i

$\delta_{y,i}$ is the yielding displacement of SDOF i (see Table 8 to Table 12)

$F_{y,i}$ is the yielding force of SDOF i (see Table 8 to Table 12)

4. Results, comments and comparisons

In the following the results are presented in detail only for PGA, PGV, PDG, Arias intensity A_I and Housner intensity H_I that are the parameters already investigated by Zanini et al. (2019) and Masi et al. (2020). Moreover the results for the Modified Acceleration Spectrum Intensity $MASI - 1$ and Modified Velocity Spectrum Intensity $MVSI - 1$ are presented too, since they showed the lowest standard deviation in our computations. The results for the relation between the mean kinematic ductility reached by the 141 SDFOs systems in the NLTHAs is also reported since it showed the lowest standard deviation between the non-linear variables. Mean kinematic ductility can also be thought as a simplified numerically assessment of the mean damage on buildings of different vulnerabilities and strengths. Only results for the max component are shown in detail since results for Res (aka $Max_{RotD100}$) component do not differ much. However, Table 6 and Table 7 show all the results for the linear and non-linear GMPs respectively.

The first two steps of the procedure proposed in section 3 allow drawing conclusion about the standard deviation to be assigned to the macroseismic intensity and to the ground motion. Distribution of values (see Figure 8 to Figure 12 for the logarithm of the selected parameters) are consistent (they do not contradict) with the assumption of uniform distribution therefore the standard deviation of the parameter σ_{I_M} can be evaluated with equation 3. The standard deviations assumed for each parameter are reported in Table 6 and Table 7. The standard deviation of the Macroseismic intensity is assumed equal to $\sigma_{I_{EMS}} = 0.85$ whereas the standard deviation of $\log(I)$ is assumed equal to $\sigma_{\log(I_{EMS})} = 0.05$. Note that once the standard deviation is evaluated for some logarithmic transformation of a ground motion parameter or of the macroseismic intensity, it can be easily converted to any other logarithmic transformation using the following equation:

	$\sigma_{\log_i x} = \frac{\sigma_{\log_j x}}{\log_j i} \quad (9)$	
--	--	--

The macroseismic intensity is the parameter that shows the highest scatter on the space variability distribution. Therefore, the suitable value of $\sigma_{EMS} = 0.85$ is higher than the value of $\sigma_{EMS} = 0.5$ assumed by previous research without clear justification (Gomez Capera et al. 2007, 2015; Faenza and Michelini 2010, 2011; Zanini et al. 2019). In fact, the approach proposed in this work assumes that the uncertainty of the measured value consists of the measurement error and the spatial factor. The latter was not taken into account in these works. The value of 0.85 value is also consistent with the usual "rule of thumb" of defining the standard deviation as 0.25 times the range value.

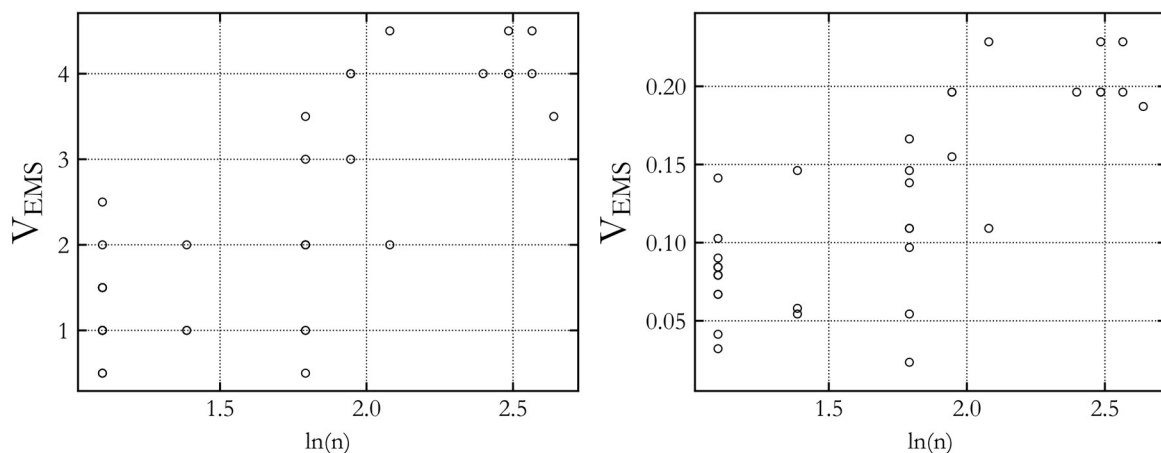


Figure 8: Distribution of the variability inside a radius of 3 km for I_{EMS} (left) $\log(I_{EMS})$ (right)

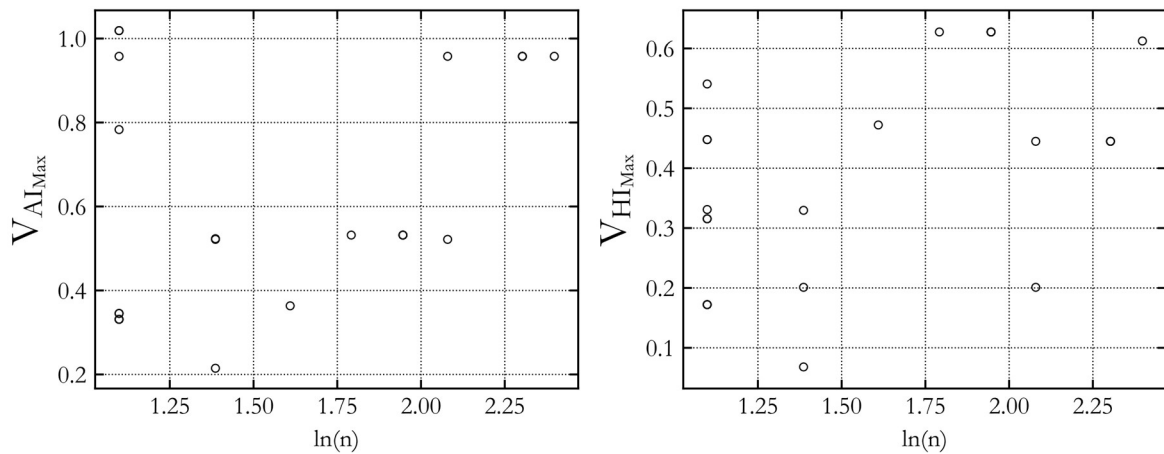


Figure 9: Distribution of the variability inside a radius of 3 km for left) Arias and right) Housner intensity

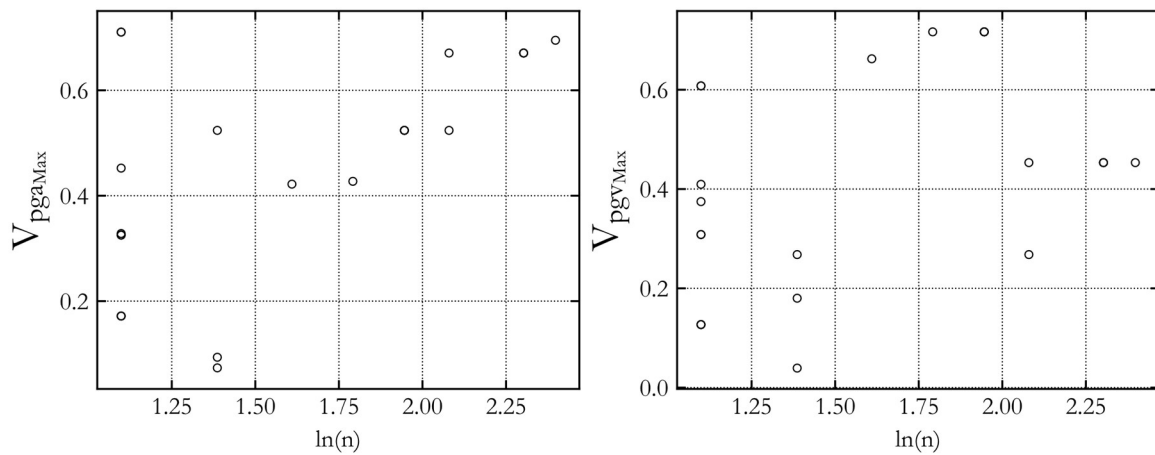


Figure 10: Distribution of the variability inside a radius of 3 km for left) PGA and right) PGV

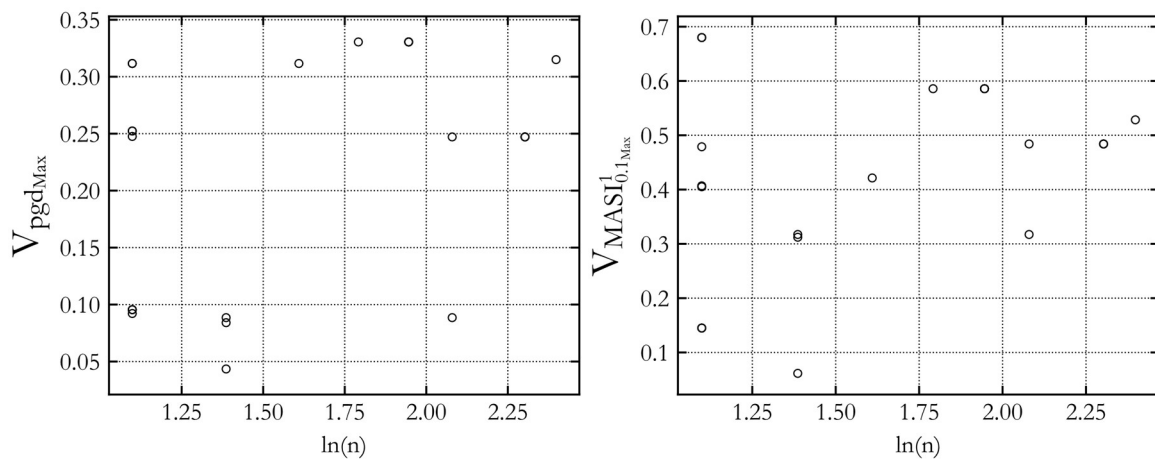


Figure 11: Distribution of the variability inside a radius of 3 km for left) PGD and right) Modified Acceleration Spectrum Intensity *MASI – 1*

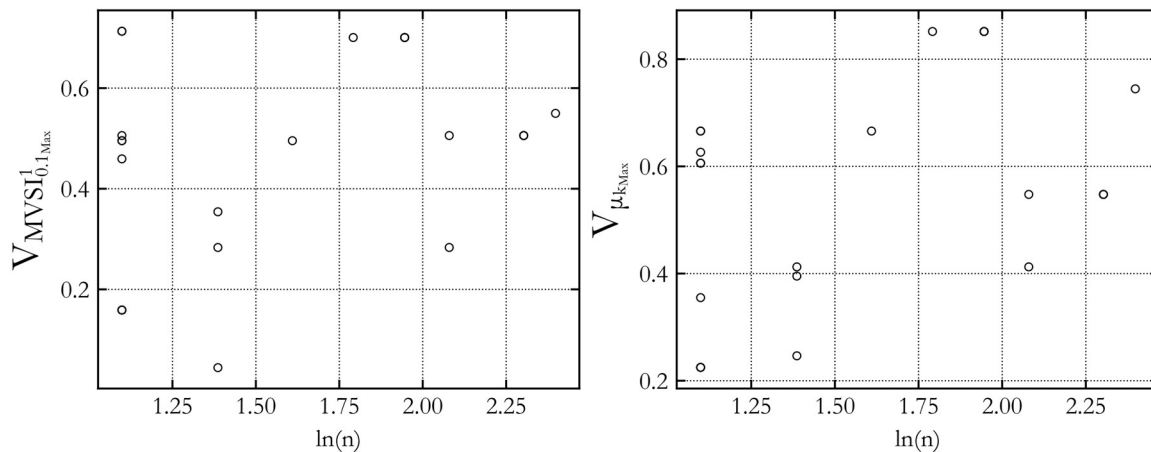


Figure 12: Distribution of the variability inside a radius of 3 km for left) Modified Velocity Spectrum Intensity *MVSI* – 1 and the kinematic ductility (right)

Using the standard deviation assumed from step 1 and 2 and reported in Table 6 and Table 7, step 3, 4 can be followed allowing to perform chi-square regression on the one-to-one database and to identify abnormal values of residuals as proposed in step 5.

Many tests have been performed to reduce the number of outliers (observations with residuals higher than 3 according to step 5) and the overall line standard deviation. Apart from trying to replicate the procedures already available in literature (then excluded for the reasons explained in section 3 and APPENDIX 1), the influence of the following parameters has been tested:

- the maximum distance between the macro data point and the recording station, using a maximum distance of 0.5, 1.5 and 3km;
- the interval for the intensity binning (0.5 or 1 degree interval);
- the influence of observation taken after repeated earthquake (seismic sequences).

These tests were conducted before arriving at the solution described here and the most significant are shown in APPENDIX 1.

Changes in the maximum distance, the adoption of a different binning size for the intensity classes (i.e. not using half degrees) or the consideration of seismic sequences did not affect much the residuals distribution and the regressions standard deviations. This fact is probably due to the uncertainties related with on field intensity assignments linked with difficulties in assessing the vulnerability class and grade of damage uniquely. Looking in the detail at the residuals distribution, the data point showing abnormal residuals suggested to change the functional form of the regression from an initial linear relation between the macroseismic intensity and the logarithm of the intensity measure *IM* to the following power law relation:

	$I = aIM^b$	(10)
--	-------------	------

As explained in section 3 this equation can be transformed in a linear relation in the natural bi-logarithmic space:

	$\ln(I) = \ln(a) + b\ln(IM)$	(11)
--	------------------------------	------

Using such form allows also to apply standard methods used in structural analysis to develop fragility functions (Zentner et al. 2017; Bakalis and Vamvatsikos 2018) and therefore it is possible to evaluate the probability that the macroseismic intensity is higher or equal to a given value given the occurrence of an intensity measure using the following relations:

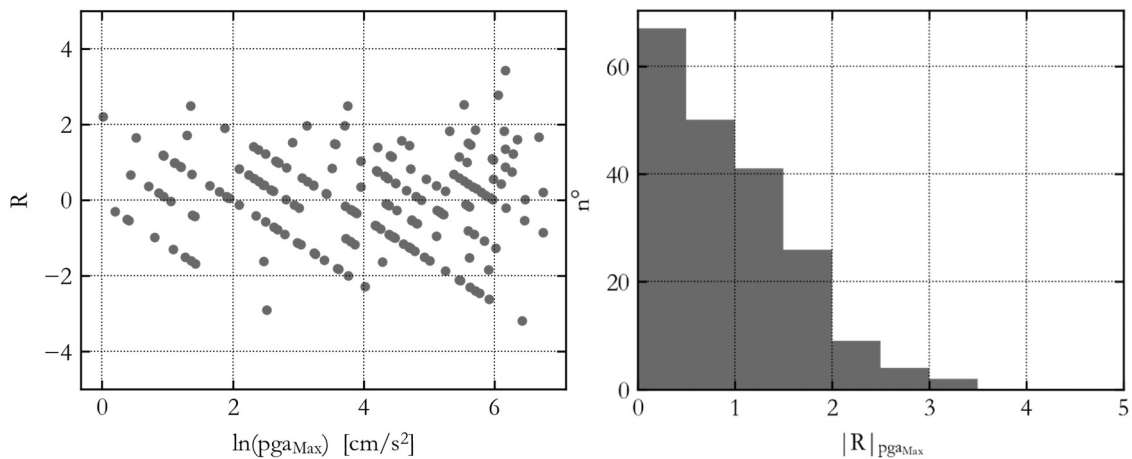
	$P[I \geq i IM] = 1 - \Phi\left(\frac{\ln(i) - \ln(a) - b \ln(IM)}{\sigma_{\ln I}}\right) \quad (12)$	
	$P[I = i IM] = P[I \geq i - 1 IM] - P[I \geq i IM] \quad (13)$	

Where Φ is the standard normal cumulative distribution function. These relations imply that residuals are normally distributed around the mean value (so given a macroseismic intensity ground motion parameters are log-normally distributed and the other way around) and that this dispersion is constant. Such hypothesis are at the base of a good regression model and are checked via the procedure already explained.

The final dataset consists in one-to-one data pairs (each MDP is linked with the closest record and the other way around) using a maximum distance of 3km between the two points. The dataset is described in Table 5.

Figure 13 to Figure 20 show the scatter plot of the selected parameters against the macroseismic intensity along with the regression line developed on the final database and the equation of the regression line. The regression coefficients developed on the final dataset for the 28 parameters are reported in APPENDIX 2, Table 6 for linear parameters and Table 7 for non-linear parameters. The regression lines for PGA, PGV, PGD, AI and Housner show values very close to those found by Zanini et al. (2019) and Masi et al. (2020) for I_{EMS} . Comparisons for pga and Housner intensity are shown in Figure 21 and Figure 22. Generally, in the present study the line standard deviations are higher. This is mainly because in the present work the regression is performed on the single data pairs whereas in Zanini et al. (2019) and Masi et al. (2020) regressions are performed on averages values per intensity classes, hence reducing the scatter around the line. However, the method suggested in this work is best suited to draw conclusions about individuals. The linear parameter that shows the best correlation is the Modified Acceleration Spectrum Intensity (MASI-1), that appear to predict I_{EMS} with a standard deviation of 0.82. The second best parameters is the Modified Velocity Spectrum Intensity (MVS1-1) predict I_{EMS} with the same standard deviation 0.82. As it can be seen from APPENDIX 2, almost all parameters show a similar behaviour suggesting that the analysis is too influenced by the uncertainties related to the intensity assignment on the field.

For consistency with the on field procedure adopted to assign macroseismic intensity, the preferred value to assess “instrumental” macroseismic intensity is the average kinematic ductility reached by the 141 different non-linear SDOF systems representing different buildings and vulnerability classes. This average kinematic ductility can predict I_{EMS} with a standard deviation of 0.80 that is comparable with standard deviations of commonly used linear GMPs.



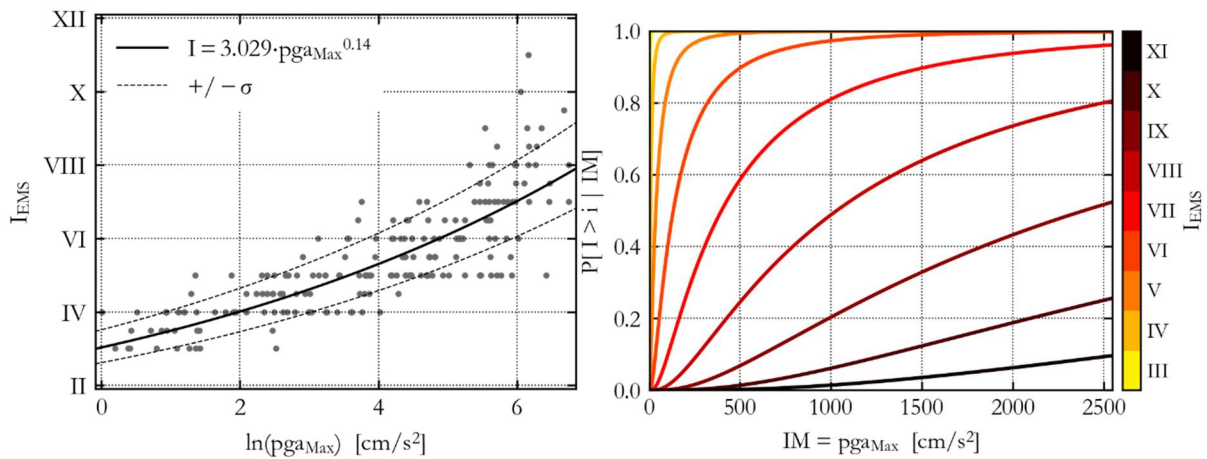


Figure 13: PGA: variation of residuals (up-left), their distribution (up-right), regression line (down-right) and “fragility” functions (down-left)

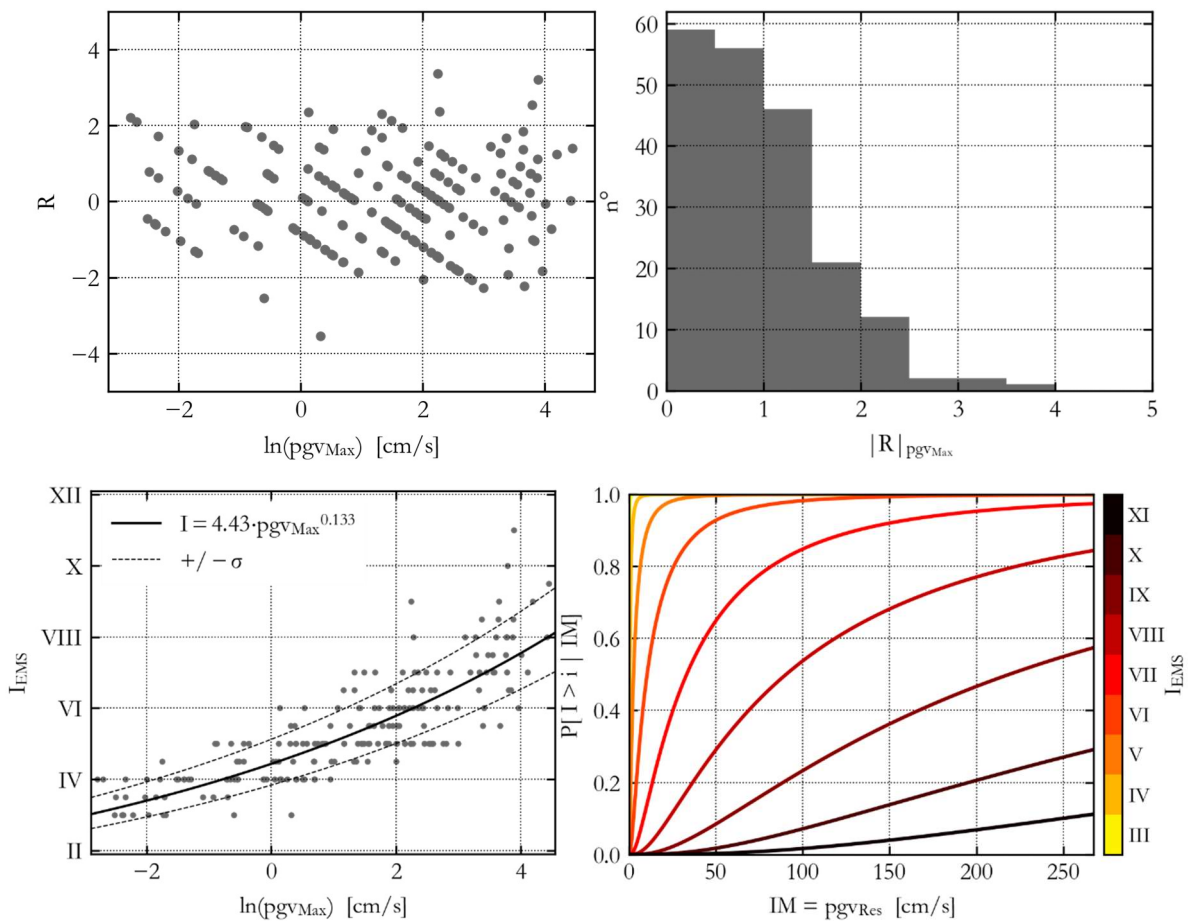


Figure 14: PGV: variation of residuals (up-left), their distribution (up-right), regression line (down-right) and “fragility” functions (down-left)

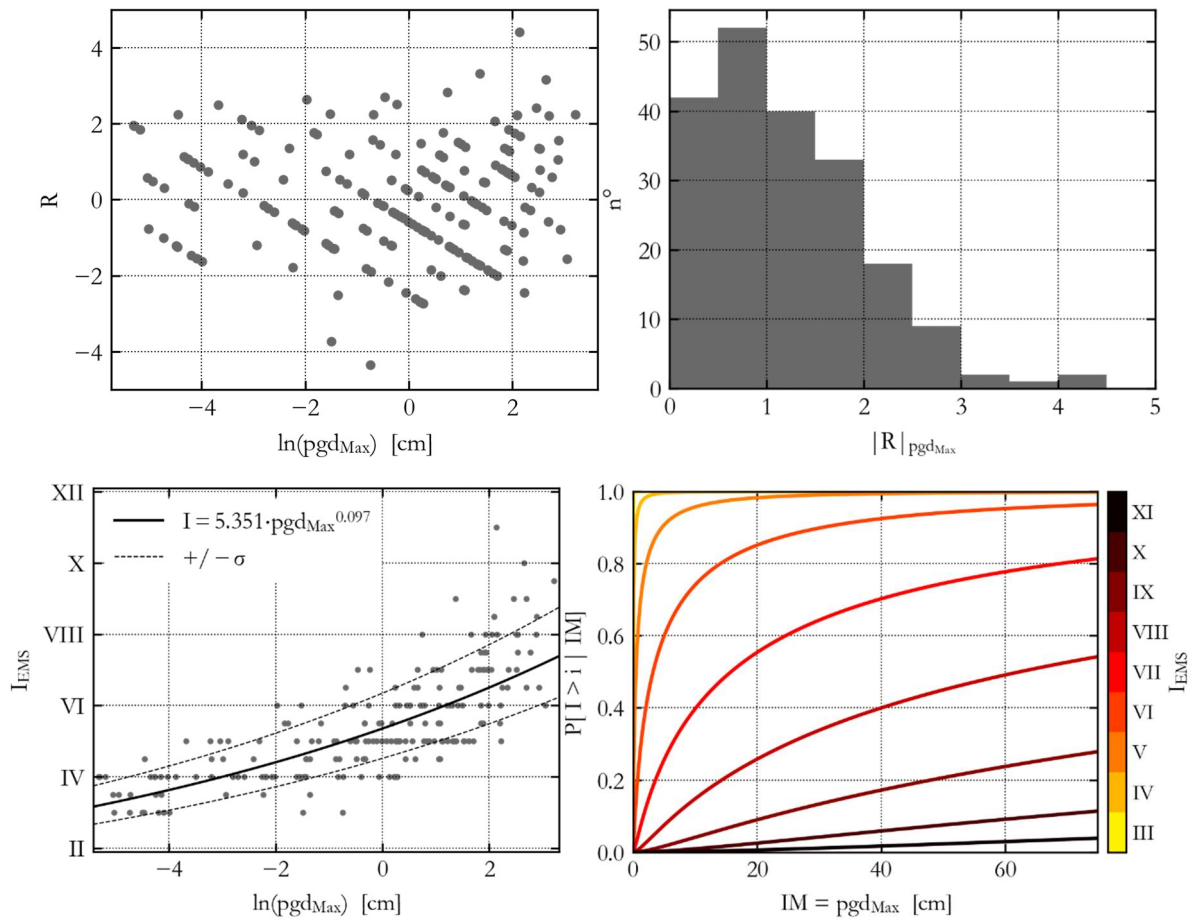
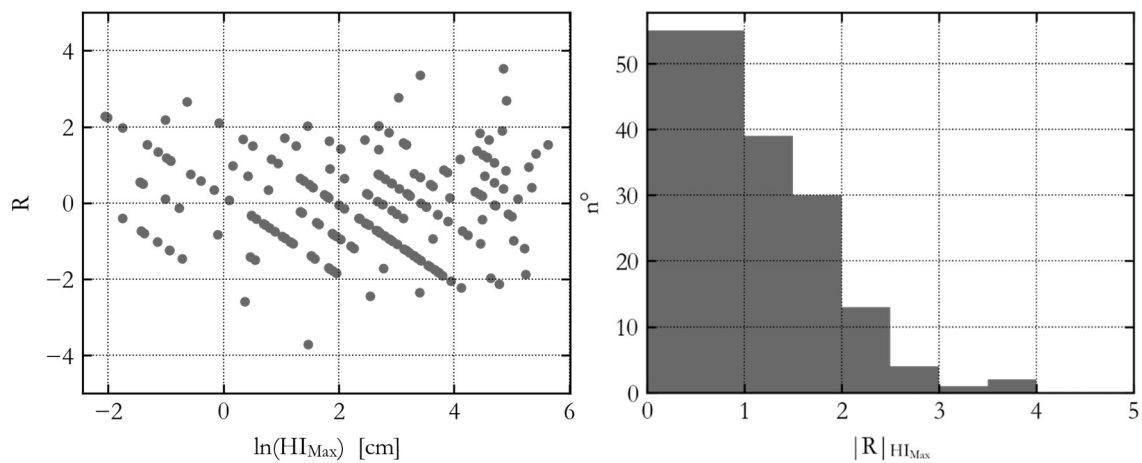


Figure 15: PGD: variation of residuals (up-left), their distribution (up- right), regression line (down- right) and “fragility” functions (down-left)



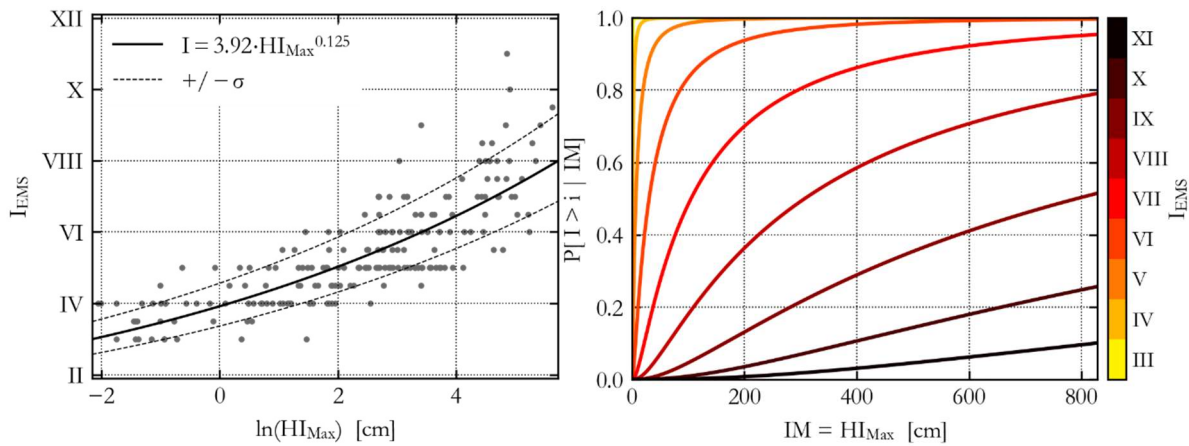


Figure 16: Housner intensity HI : variation of residuals (up-left), their distribution (up-right), regression line (down-right) and “fragility” functions (down-left)

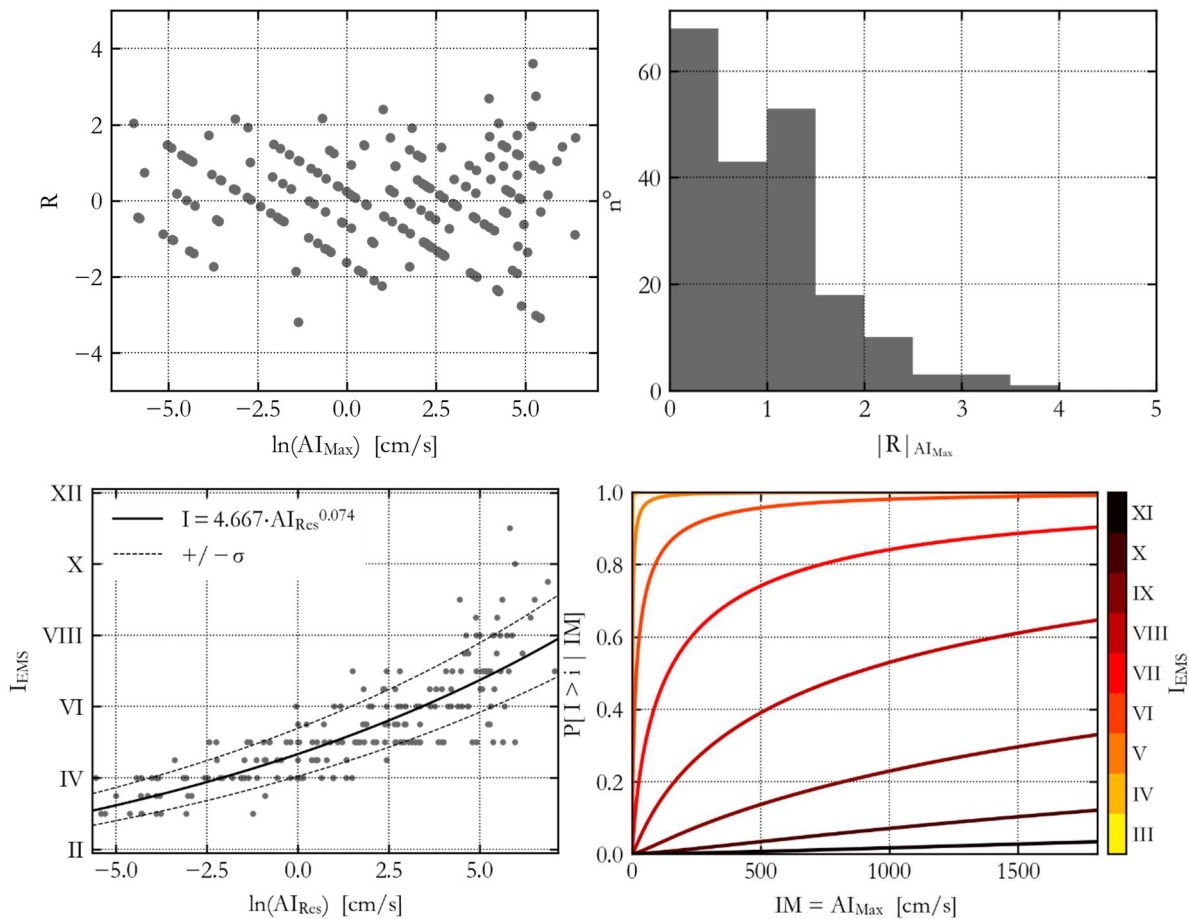


Figure 17: Arias intensity AI : variation of residuals (up-left), their distribution (up-right), regression line (down-right) and “fragility” functions (down-left)

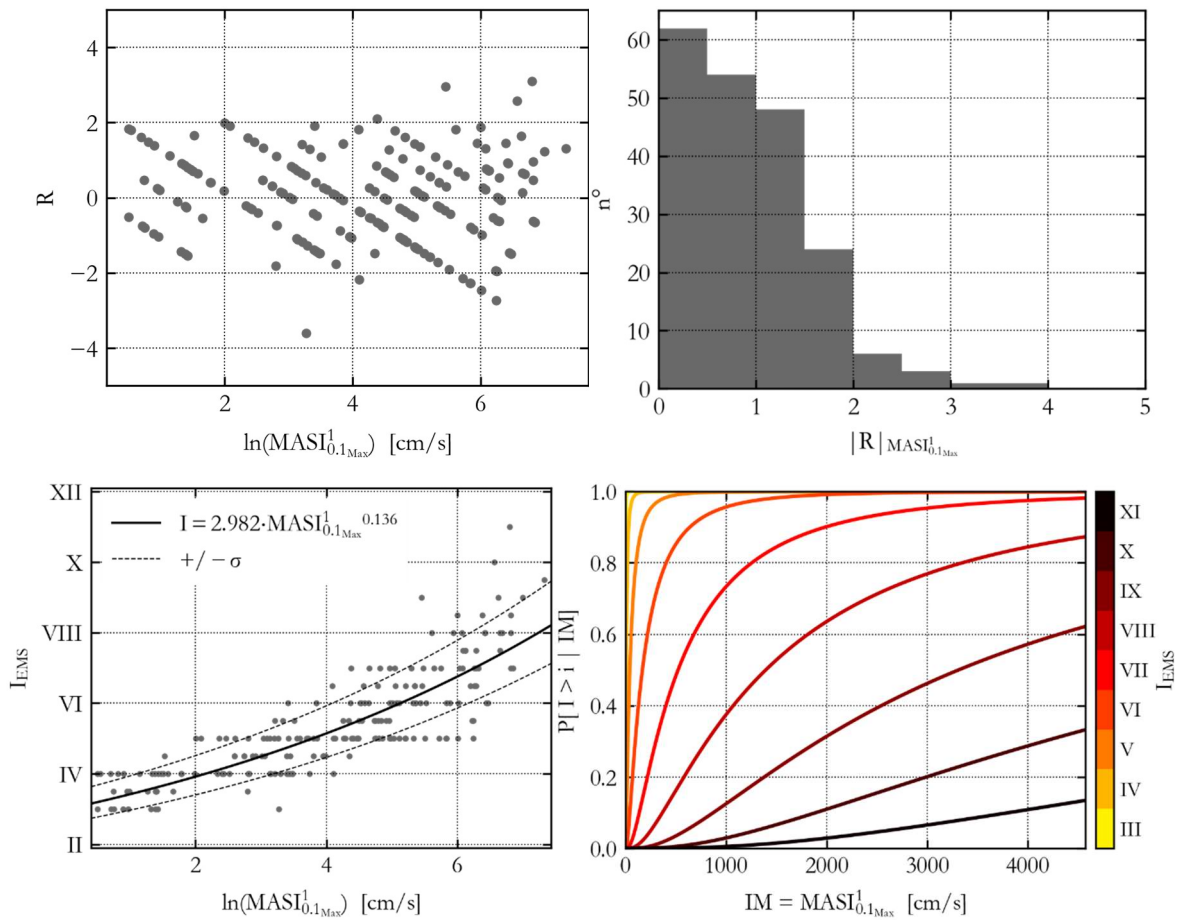
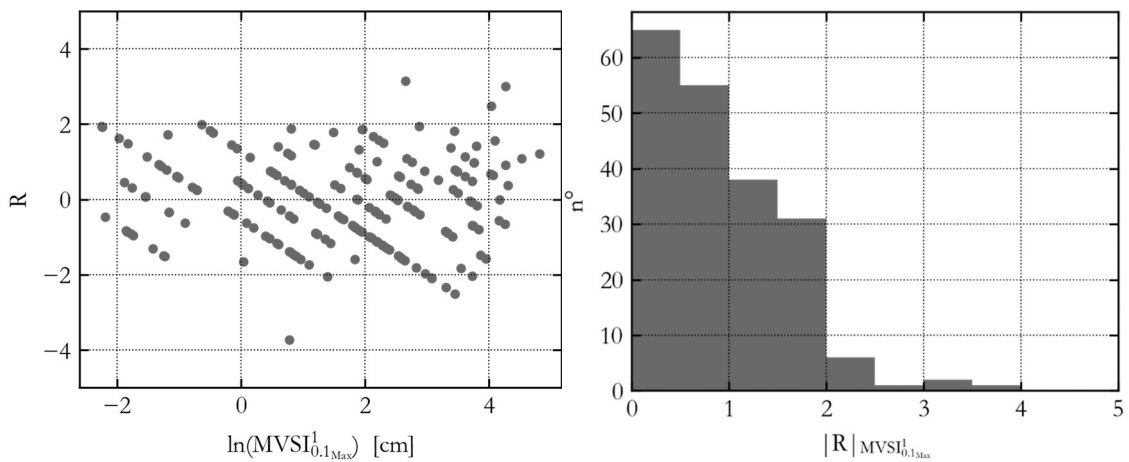


Figure 18: Modified Acceleration Spectrum Intensity *MASI* – 1: variation of residuals (up-left), their distribution (up- right), regression line (down-right) and “fragility” functions (down-left)



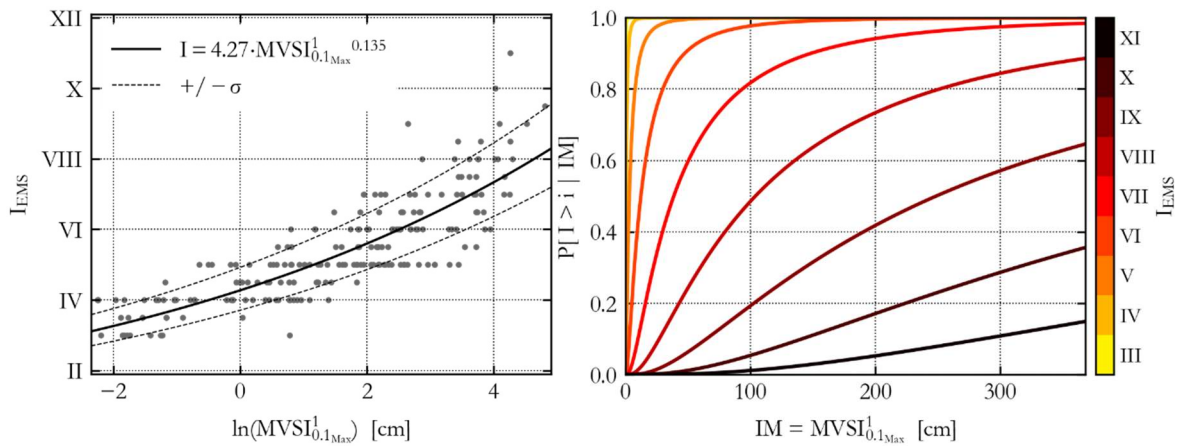


Figure 19: Modified Velocity Spectrum Intensity $MVSI - 1$: variation of residuals (up-left), their distribution (up-right), regression line (down-right) and “fragility” functions (down-left)

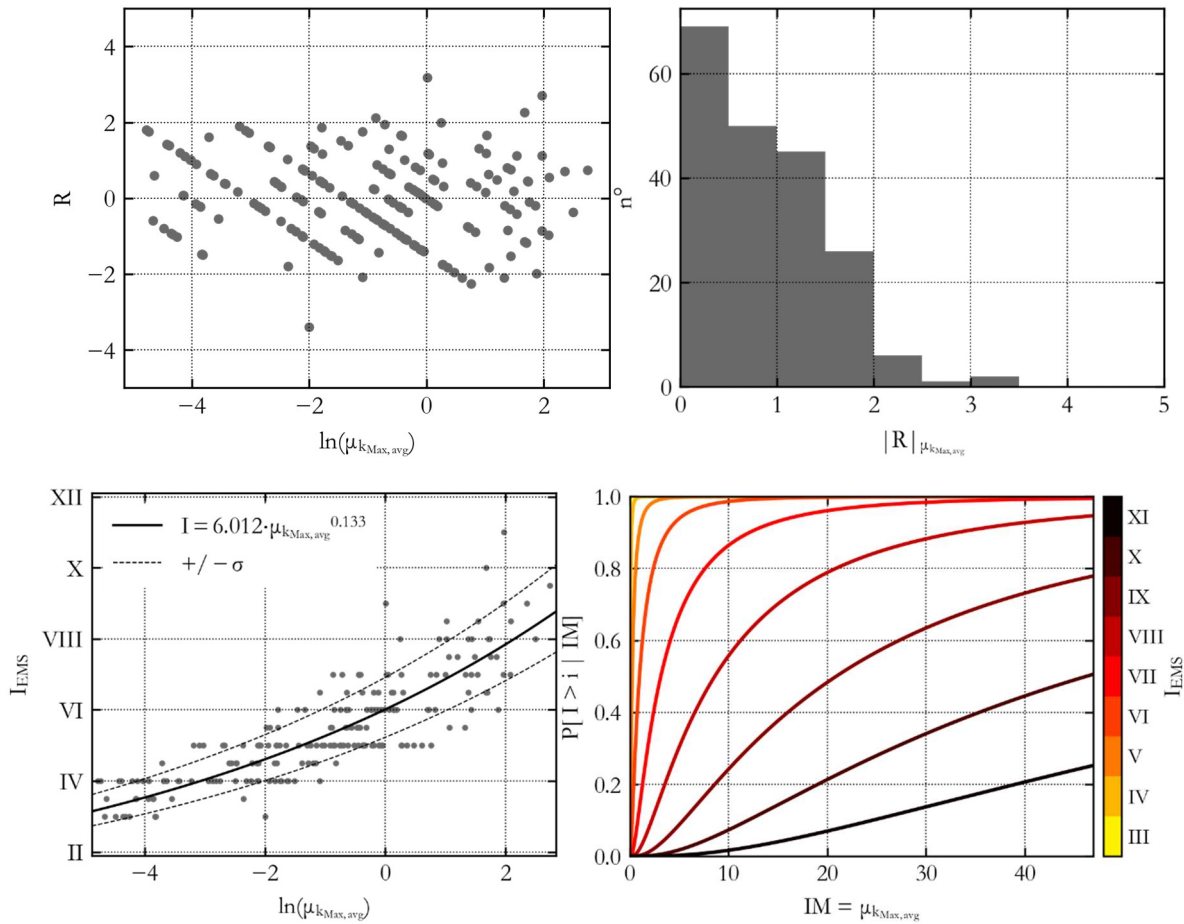


Figure 20: Kinematic ductility μ_{max} : variation of residuals (up-left), their distribution (up-right), regression line (down-right) and “fragility” functions (down-left)

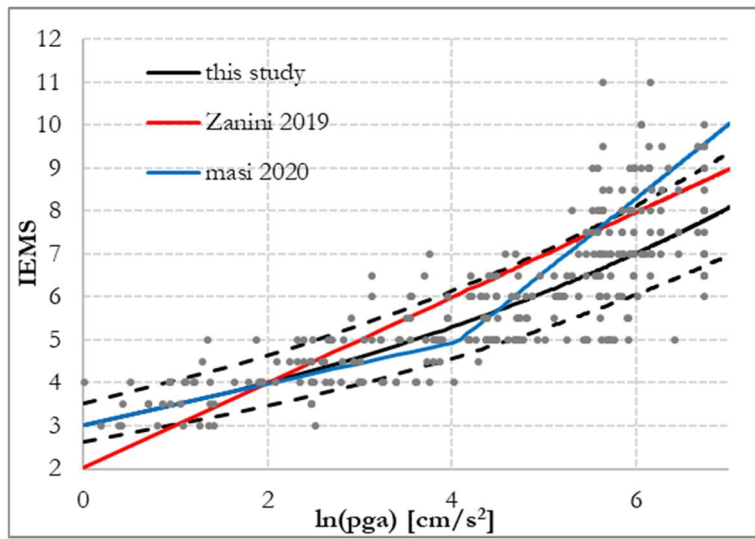


Figure 21: PGA: comparisons between results of this study and published ones

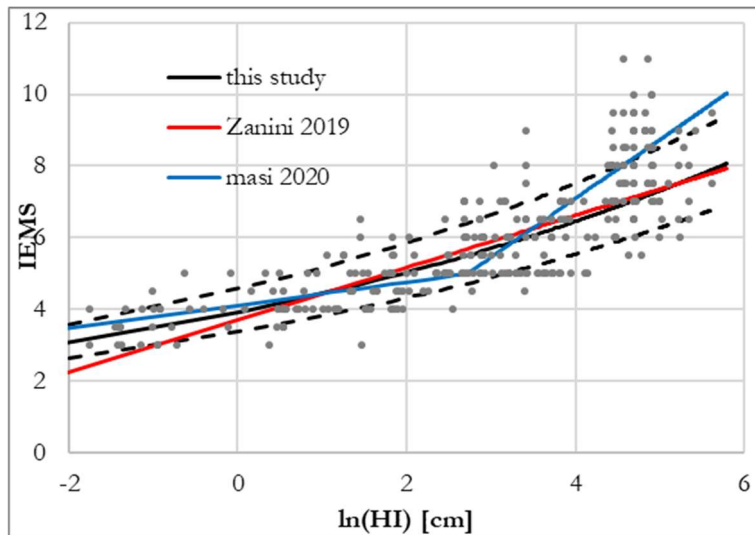


Figure 22: Housner intensity: comparisons between results of this study and published ones

Table 5: Characteristics of the final database

ID	Date	Lat	Lon	Depth	M _w	M _L	N° I-MDP
IT-1976-0002	06/05/1976	46.262	13.3	5.7	6.4	6.4	4
IT-1983-0004	20/07/1983	37.5487	15.168	24.7	4.5	4.3	1
IT-1984-0004	07/05/1984	41.7	13.86	20.5	5.9	5.9	10
IT-1999-0012	14/02/1999	38.183	15.019	12	4.7	3.9	1
IT-2001-0008	22/04/2001	37.702	15.02	5	4.2	3.2	1
IT-2002-0007	05/04/2002	38.352	15.096	5	4.4	4.2	1
IT-2002-0024	06/09/2002	38.381	13.701	5	5.8	5.6	3
IT-2002-0040	27/10/2002	37.76	15.116	5	4.9	4.8	1
IT-2003-0048	14/09/2003	44.255	11.38	8.3	5.3	5.0	2
IT-2006-0059	27/02/2006	38.155	15.2	9.2	4.4	4.1	6
IT-2006-0302	19/12/2006	37.778	14.913	23.8	4.2	4.1	2
IT-2009-0009	06/04/2009	42.342	13.38	8.3	6.1	5.9	4
IT-2009-0317	08/11/2009	37.847	14.557	7.6	4.4	4.4	1
IT-2009-0323	15/12/2009	43.007	12.271	8.8	4.2	4.3	1
IT-2009-0328	19/12/2009	37.782	14.974	26.9	nan	4.4	6
ISIDe-2166809	02/04/2010	37.799	15.079	0.3	nan	4.3	1
IT-2010-0032	16/08/2010	38.352	14.894	13.5	4.7	4.8	1
EMSC-20110506_0000042	06/05/2011	37.804	14.943	20.4	4.3	4.0	1
IT-2011-0110	23/06/2011	38.064	14.784	7.3	4.5	4.4	7
IT-2011-0020	17/07/2011	45.01	11.367	2.4	4.8	4.8	3
IT-2011-0022	25/07/2011	45.016	7.365	11	4.3	4.3	4
IT-2012-0002	25/01/2012	44.871	10.51	29	5.0	5.0	3
IT-2012-0008	20/05/2012	44.8955	11.2635	9.5	6.1	5.9	1
IT-2012-0011	29/05/2012	44.8417	11.0657	8.1	6.0	5.8	21
IT-2012-0061	25/10/2012	39.8747	16.0158	9.7	nan	5.0	13
IT-2013-0001	04/01/2013	37.881	14.719	9.6	4.3	4.4	2
IT-2013-0005	21/06/2013	44.1308	10.1357	7	5.1	5.2	2
IT-2013-0013	15/08/2013	38.111	14.913	19.4	nan	4.5	5
EMSC-20160824_0000006	24/08/2016	42.6983	13.2335	8.1	6.0	6.0	17
EMSC-20161026_0000095	26/10/2016	42.9087	13.1288	7.5	5.9	5.9	15
EMSC-20161030_0000029	30/10/2016	42.8322	13.1107	9.2	6.5	6.1	59

5. Conclusions

The present work analysed the relation between Ground Motion Parameters and macroseismic intensity assigned using the European Macroseismic Scale. A database is constructed matching available ground motion and macroseismic data and regressions using chi-square regression are conducted on 28 different parameters. The work proposes a methodology to assign “instrumental” macroseismic intensity trying to simulate numerically the procedure employed on field for the assessment of the macroseismic intensity. Finally, regression equations are proposed in order to assign an instrumental macroseismic intensity to a recorded accelerogram. The peculiarity of the proposed approach to regression relations is as follows: we assume that the uncertainty of the studied values includes both measurement errors and the spatial factor. The latter was not taken into account in previous works. The records included in the final database and classified according to the macroseismic intensity are 199 deriving from 31 different earthquakes. Moment magnitude ranges from 4.2 to 6.5. Figure 23 shows the Magnitude vs Epicentral distance distribution of the records included in the final dataset and the distribution of couples for each intensity degree arranged in bins with half-degree width. Macroseismic intensity ranges from $I_{EMS}=III$ to $I_{EMS}=XI$. Figure 24 shows the distribution of the distances between the MDPs and the station and the distribution of magnitudes among the observed MDPs which is almost constant.

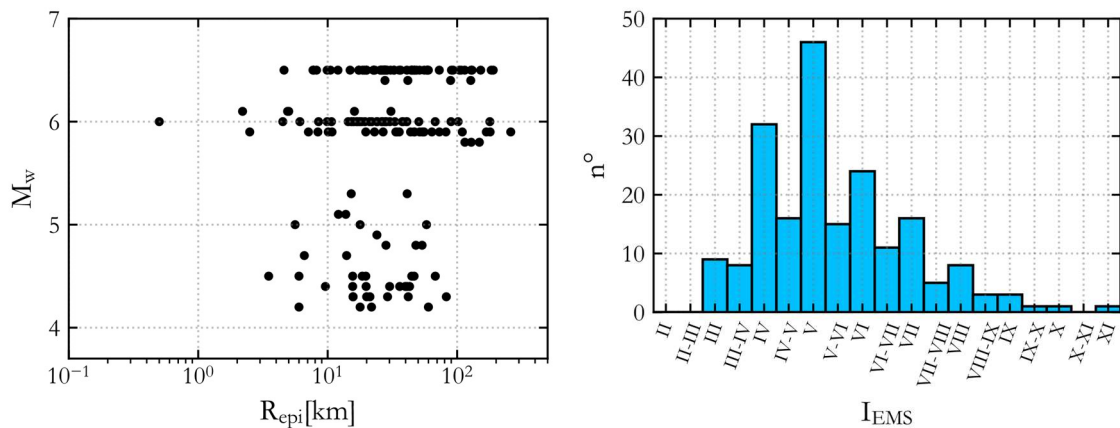


Figure 23: Magnitude vs Epicentral distance of the records included in the final dataset (left) and Distribution of couples MDP-record for each intensity degree (right)

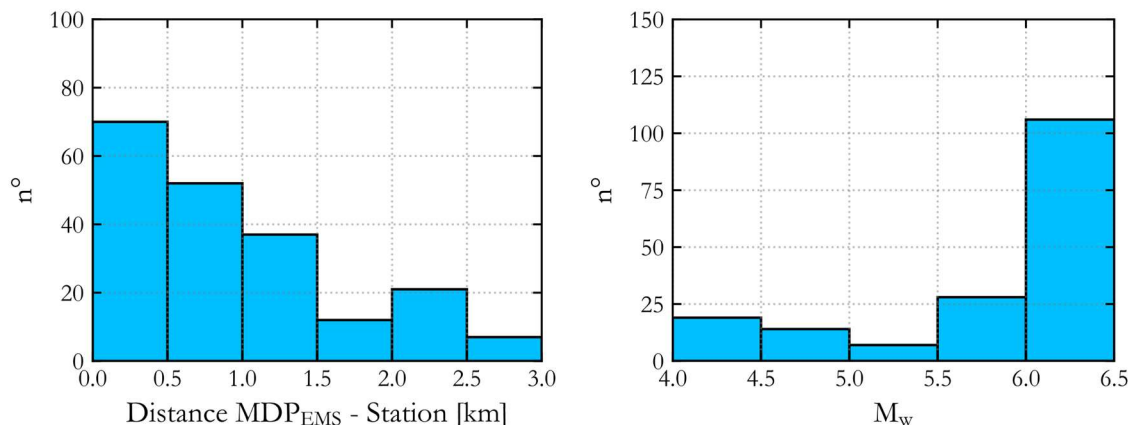


Figure 24: Distribution of the distance MDP-station of the recorded the accelerogram (left) and Distribution of couples MDP-record for different magnitude ranges present in the final dataset (right)

Bibliography

- Anderson JC, Bertero V V. (1987) Uncertainties in Establishing Design Earthquakes. *Journal of Structural Engineering* 113:1709–1724. doi: 10.1061/(ASCE)0733-9445(1987)113:8(1709)
- Azzaro R, Barbano MS, D'Amico S, et al (2011) The L'Aquila 2009 earthquake: An application of the European Macroseismic Scale to the damage survey in the epicentral area. *Bollettino di Geofisica Teorica ed Applicata* 52:561–581. doi: 10.4430/bgta0012
- Bakalis K, Vamvatsikos D (2018) Seismic Fragility Functions via Nonlinear Response History Analysis. *Journal of Structural Engineering (United States)* 144:1–15. doi: 10.1061/(ASCE)ST.1943-541X.0002141
- Bilal M, Askan A (2014) Relationships between Felt Intensity and Recorded Ground-Motion Parameters for Turkey. *Bulletin of the Seismological Society of America* 104:484–496. doi: 10.1785/0120130093
- Caprio M, Tarigan B, Bruce Worden C, et al (2015) Ground motion to intensity conversion equations (GMICES): A global relationship and evaluation of regional dependency. *Bulletin of the Seismological Society of America* 105:1476–1490. doi: 10.1785/0120140286
- Cornell BYCA (1968) Engineering Seismic Risk Analysis. *Bulletin of the Seismological Society of America* 58:1583–1606
- Faenza L, Michelini A (2010) Regression analysis of MCS intensity and ground motion parameters in Italy and its application in ShakeMap. *Geophysical Journal International* 180:1138–1152. doi: 10.1111/j.1365-246X.2009.04467.x
- Faenza L, Michelini A (2011) Regression analysis of MCS intensity and ground motion spectral accelerations (SAs) in Italy. *Geophysical Journal International* 186:1415–1430. doi: 10.1111/j.1365-246X.2011.05125.x
- Gomez Capera AA, Albarello D, Gasperini P (2007) Aggiornamento relazioni fra l'intensità macrosismica e PGA
- Gomez Capera AA, Locati M, Luzi L, et al (2015) Macroseismic and ground motion : site specific conversion rules - Relationships between GM and macroseismic Intensity for Italy
- Graziani L, del Mese S, Tertulliani A, et al (2019) Investigation on damage progression during the 2016–2017 seismic sequence in Central Italy using the European Macroseismic Scale (EMS-98). *Bulletin of Earthquake Engineering*. doi: 10.1007/s10518-019-00645-w
- Graziani L, Tertulliani A, Maramai A, et al (2017) The 7 and 11 May 1984 earthquakes in Abruzzo-Latium (Central Italy): reappraisal of the existing macroseismic datasets according to the EMS98. *Journal of Seismology* 21:1219–1227. doi: 10.1007/s10950-017-9663-3
- Grimaz S, Malisan P (2017) How could cumulative damage affect the macroseismic assessment? *Bulletin of Earthquake Engineering* 15:2465–2481. doi: 10.1007/s10518-016-0016-3
- Grünthal G (1998) European Macroseismic Scale 1998
- Ibarra LF, Medina RA, Krawinkler H (2005) Hysteretic models that incorporate strength and stiffness deterioration. *Earthquake Engineering & Structural Dynamics* 34:1489–1511. doi: 10.1002/eqe.495
- Klügel J-U, Stäuble-Akcay S (2018) Towards damage-consistent performance-based design of critical infrastructures. *International Journal of Computational Methods and Experimental Measurements* 6:933–943. doi: 10.2495/cmcm-v6-n5-933-943
- Lagomarsino S, Giovinazzi S (2006) Macroseismic and mechanical models for the vulnerability and damage assessment of current buildings. *Bulletin of Earthquake Engineering* 4:415–443. doi: 10.1007/s10518-006-9024-z
- Lanzano G, Sgobba S, Luzi L, et al (2019) The pan-European Engineering Strong Motion (ESM) flatfile: compilation criteria and data statistics. *Bulletin of Earthquake Engineering* 17:561–582. doi: 10.1007/s10518-018-0480-z
- Locati M, Camassi R, Rovida A, et al (2016) Database Macrosismico Italiano , versione DBMI15

- Lolli B, Gasperini P (2012) A comparison among general orthogonal regression methods applied to earthquake magnitude conversions. *Geophysical Journal International* 190:1135–1151. doi: 10.1111/j.1365-246X.2012.05530.x
- Masi A, Chiauzzi L, Nicodemo G, Manfredi V (2020) Correlations between macroseismic intensity estimations and ground motion measures of seismic events. Springer Netherlands
- Mouroux P, Brun B Le (2006) Presentation of RISK-UE Project. *Bulletin of Earthquake Engineering* 4:323–339. doi: 10.1007/s10518-006-9020-3
- Musson RMW, Grünthal G, Stucchi M (2010) The comparison of macroseismic intensity scales. *Journal of Seismology* 14:413–428. doi: 10.1007/s10950-009-9172-0
- Park Y, Ang AH -S., Wen YK (1985) Seismic Damage Analysis of Reinforced Concrete Buildings. *Journal of Structural Engineering* 111:740–757. doi: 10.1061/(ASCE)0733-9445(1985)111:4(740)
- Reed JW, Kassawara RP (1990) A criterion for determining exceedance of the operating basis earthquake. *Nuclear Engineering and Design* 123:387–396. doi: 10.1016/0029-5493(90)90259-Z
- Rossi A, Tertulliani A, Azzaro R, et al (2019) The 2016–2017 earthquake sequence in Central Italy: macroseismic survey and damage scenario through the EMS-98 intensity assessment. *Bulletin of Earthquake Engineering* 17:2407–2431. doi: 10.1007/s10518-019-00556-w
- Tertulliani A, Arcoraci L, Berardi M, et al (2012) The Emilia 2012 sequence: A macroseismic survey. *Annals of Geophysics* 55:679–687. doi: 10.4401/ag-6140
- Tertulliani A, Cčić I, Meurers R, et al (2018) The 6 May 1976 Friuli earthquake: Re-evaluating and consolidating transnational macroseismic data. *Bollettino di Geofisica Teorica ed Applicata* 59:417–444. doi: 10.4430/bgta0234
- Tselentis G-A, Danciu L (2008) Empirical Relationships between Modified Mercalli Intensity and Engineering Ground-Motion Parameters in Greece. *Bulletin of the Seismological Society of America* 98:1863–1875. doi: 10.1785/0120070172
- Zanini MA, Hofer L, Faleschini F (2019) Reversible ground motion-to-intensity conversion equations based on the EMS-98 scale. *Engineering Structures* 180:310–320. doi: 10.1016/j.engstruct.2018.11.032
- Zentner I, Gündel M, Bonfils N (2017) Fragility analysis methods: Review of existing approaches and application. *Nuclear Engineering and Design* 323:245–258. doi: 10.1016/j.nucengdes.2016.12.021

APPENDIX 1 Performed tests

This appendix briefly shows the results of the most meaningful tests that were performed to reach the final regressions proposed in section 4. The following functional forms were tested for the regression equation:

a)	$I = a + b \ln(IM)$	(14)
b)	$I = aIM^b$	(15)

a) Test on binned data (following available literature)

In these tests data were binned according to their macroseismic intensity following the procedure suggest by Faenza and Michelini (2010). Standard deviation used to perform the chi-square regression (equivalent to ODR) were assumed equal to the standard deviation of the different bins for the ground motion parameters and to 0.5 for the macroseismic intensity.

Results are reported only for the kinematic ductility which is the final parameter selected for the purposes of this study. Both Figure 25 and Figure 26 show some heteroscedasticity. Moreover it is clear from the pictures that not all intensities are equally represented. Therefore, inferring the standard deviation of the ground motion parameters from the variability found inside each beam is questionable, For higher intensities the variability looks lower only because of the scarcity of data.

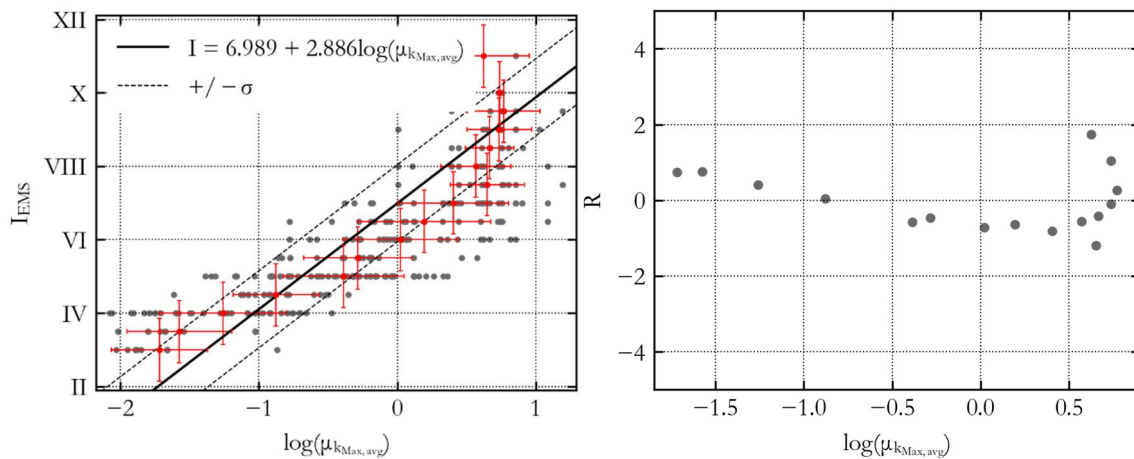


Figure 25: Test on binned data – equation a: Kinematic ductility μ_{max} : regression line (left) and variation of residuals (right)

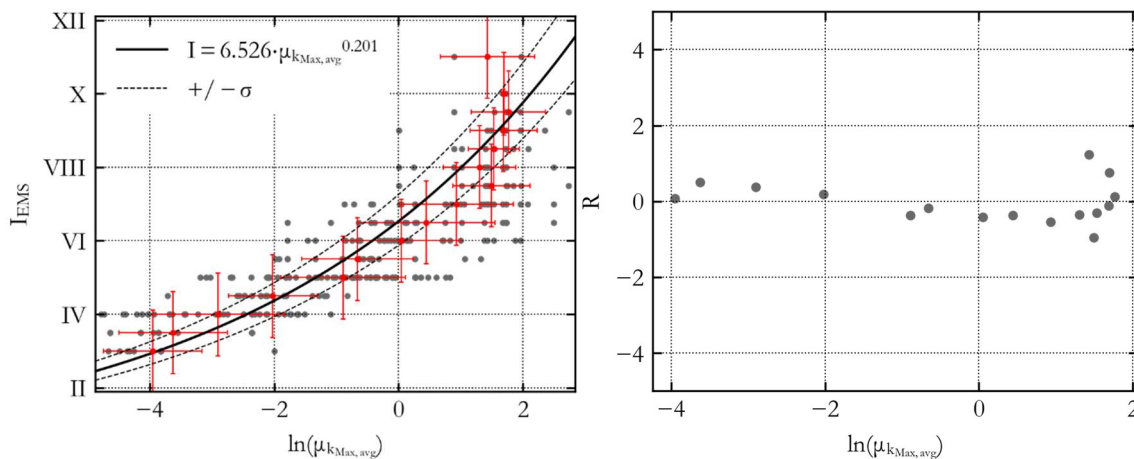


Figure 26: Test on binned data – equation b: Kinematic ductility μ_{max} : regression line (left) and variation of residuals (right)

b) Tests on the maximum distance

The maximum distance between the macrodata point and the recording station is usually set equal to 3km. This number is chosen conventionally since it can represent the average length of a village or a uniform area where the macroseismic intensity is assessed. The influence of this distance in the residuals and regression lines was investigated reducing it to 0.5 km building a one-to-one database. Results, reported in Figure 27 and Figure 28, do not show a clear and significant influence of the distance on the regression lines and residuals that are still characterized by a standard deviation higher (even if very close) than that of the selected model reported in section 4.

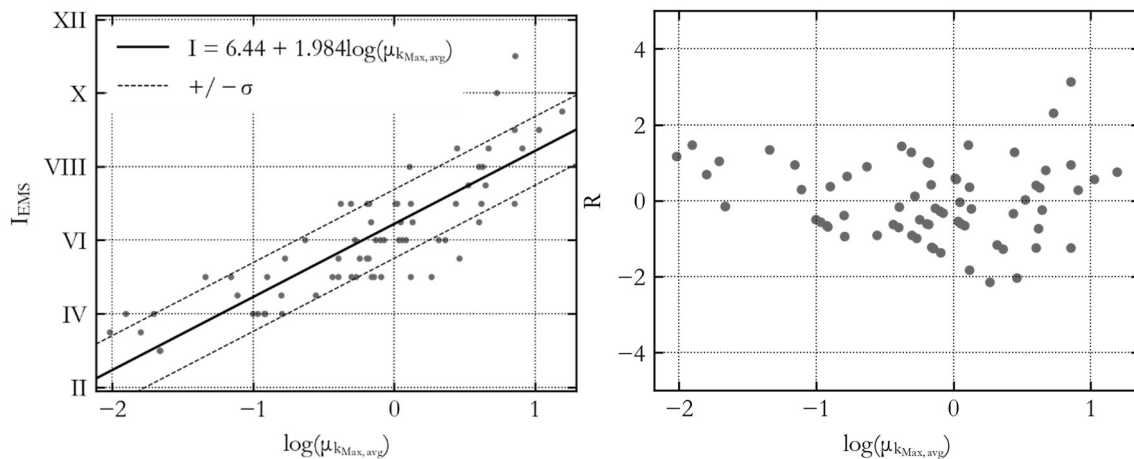


Figure 27: Test on max distance = 0.5 km – equation a: Kinematic ductility μ_{max} : regression line (left) and variation of residuals (right)

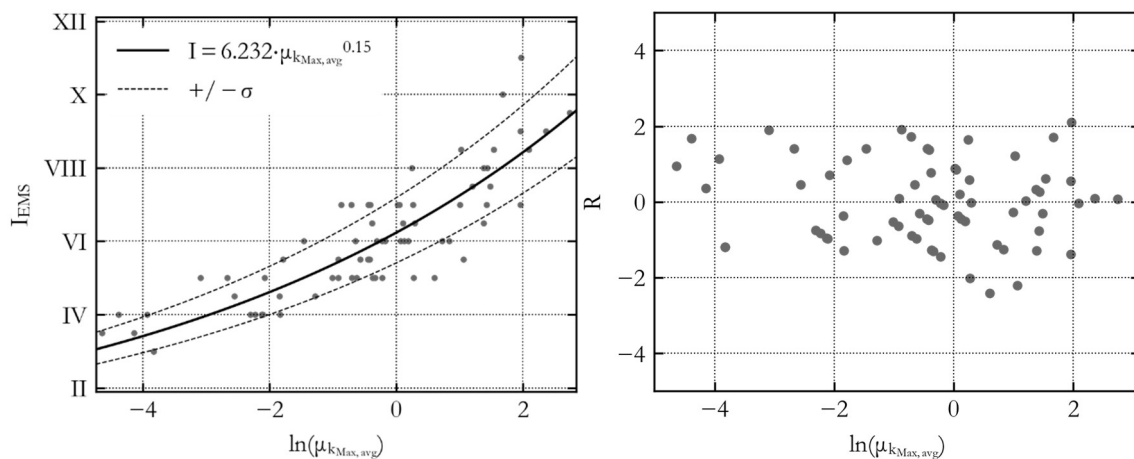


Figure 28: Test on max distance = 0.5 km – equation b: Kinematic ductility μ_{max} : regression line (left) and variation of residuals (right)

c) Test excluding seismic sequences

The macroseismic intensity should be, in principle, strongly affected by seismic sequences therefore we tried to account for this fact removing the central Italy event of the 26/10 and 30/10/2016 and the second Emilian shock of 2012. Moreover, for these events, where also the records from the previous shocks were available, the average kinematic ductility was evaluated using the entire seismic sequence as a single record (records from different earthquakes were put one after the other). However residuals still show little heteroscedasticity and the maximum intensity in the database, because of the removal of several records, goes down to XIII reducing the applicability of the proposed equations.



APPENDIX 2 Regression coefficients for the GMPs

This appendix reports all the regression coefficients calculated on the final database for the 28 ground motion parameters.

Table 6: Linear GMPs: parameter, parameter standard deviation, regression coefficients a and b, standard deviation of the predicted intensity (logarithmic and normal) and of the predicted parameter (inverse equation) and average of residuals

IM	$\sigma_{In(IM)}$	a	b	$\sigma_{In(I)}$	σ_I	$\sigma_{In(IM)}$	R_{avg}
pgaRes	0.345	3.002	0.140	0.147	0.860	1.052	-0.00005
pgaMax	0.345	3.029	0.140	0.147	0.862	1.051	0.00000
pgvRes	0.299	4.389	0.133	0.143	0.825	1.072	0.00006
pgvMax	0.299	4.430	0.133	0.145	0.836	1.087	-0.00001
pgdRes	0.161	5.308	0.097	0.170	0.981	1.755	0.00002
pgdMax	0.161	5.351	0.097	0.170	0.979	1.747	0.00001
ariasRes	0.437	4.667	0.074	0.144	0.851	1.955	-0.00004
ariasMax	0.461	4.865	0.074	0.144	0.852	1.961	-0.00012
cavRes	0.207	2.327	0.151	0.157	0.916	1.036	0.00004
cavMax	0.207	2.470	0.151	0.157	0.915	1.038	-0.00002
cadRes	0.207	3.659	0.117	0.183	1.050	1.557	0.00004
cadMax	0.184	3.839	0.116	0.183	1.049	1.571	0.00007
SEDRes	0.461	4.293	0.064	0.162	0.926	2.539	0.00000
SEDMax	0.461	4.447	0.063	0.162	0.928	2.560	0.00000
armsRes	0.253	4.000	0.146	0.143	0.847	0.978	0.00003
armsMax	0.276	4.164	0.146	0.143	0.848	0.980	0.00002
vrmsRes	0.230	5.669	0.132	0.154	0.883	1.167	0.00000
vrmsMax	0.230	5.866	0.131	0.154	0.885	1.177	0.00004
drmsRes	0.184	6.190	0.092	0.180	1.036	1.953	-0.00004
drmsMax	0.184	6.317	0.091	0.180	1.033	1.967	0.00001
IcRes	0.345	3.226	0.098	0.142	0.844	1.449	-0.00003
IcMax	0.368	3.361	0.098	0.143	0.845	1.453	-0.00002
MIVRes	0.299	4.034	0.137	0.144	0.830	1.052	0.00000
MIVMax	0.322	4.163	0.137	0.145	0.839	1.063	-0.00004
MIDRes	0.184	5.066	0.097	0.175	1.008	1.806	0.00005
MIDMax	0.184	5.173	0.096	0.175	1.005	1.821	0.00002
housnerRes	0.276	3.855	0.124	0.152	0.868	1.217	-0.00004
housnerMax	0.299	3.920	0.125	0.153	0.876	1.225	-0.00002
M_H1Res	0.322	4.236	0.134	0.142	0.813	1.060	0.00001
M_H1Max	0.322	4.312	0.133	0.143	0.819	1.073	0.00000
M_H15Res	0.299	3.960	0.134	0.142	0.820	1.063	0.00003
M_H15Max	0.322	4.019	0.134	0.143	0.824	1.063	0.00000
ASIRes	0.299	3.144	0.136	0.146	0.854	1.069	0.00002
ASIMax	0.322	3.191	0.137	0.147	0.859	1.070	0.00006
M_AS11Res	0.299	2.924	0.137	0.141	0.816	1.030	0.00000
M_AS11Max	0.299	2.982	0.136	0.142	0.821	1.039	-0.00002

M_ASI15Res	0.276	2.866	0.135	0.141	0.817	1.040	0.00001
M_ASI15Max	0.299	2.914	0.136	0.142	0.823	1.045	-0.00006
VSIRes	0.276	3.702	0.131	0.146	0.842	1.110	-0.00003
VSIMax	0.299	3.750	0.132	0.146	0.847	1.108	0.00005
M_VSI1Res	0.322	4.199	0.136	0.141	0.812	1.040	0.00001
M_VSI1Max	0.322	4.270	0.135	0.142	0.816	1.048	-0.00005
M_VSI15Res	0.299	3.960	0.134	0.142	0.820	1.063	0.00003
M_VSI15Max	0.322	4.019	0.134	0.143	0.824	1.063	0.00000
ESI05Res	0.576	8.067	0.075	0.145	0.862	1.946	-0.00003
ESI05Max	0.576	8.411	0.076	0.146	0.872	1.934	-0.00002
ESI1Res	0.622	7.445	0.073	0.144	0.830	1.975	-0.00002
ESI1Max	0.622	7.717	0.073	0.145	0.837	1.980	-0.00002
ESI15Res	0.576	7.186	0.071	0.147	0.847	2.071	0.00002
ESI15Max	0.599	7.467	0.072	0.147	0.853	2.046	-0.00002

Table 7: Non-Linear GMPs: parameter, parameter standard deviation, regression coefficients a and b, standard deviation of the predicted intensity (normal and logarithmic) and of the predicted parameter (inverse equation) and average of residuals

IM	$\sigma_{\ln(IM)}$	a	b	$\sigma_{\ln(I)}$	σ_I	$\sigma_{\ln(IM)}$	R_{avg}
d_kinRes	0.368	5.954	0.133	0.139	0.796	1.045	0.00001
d_cycRes	0.368	5.954	0.133	0.139	0.796	1.045	0.00001
d_hystRes	0.484	4.371	0.242	0.201	1.166	0.829	-0.00005
d_kinMax	0.391	6.012	0.133	0.140	0.801	1.052	-0.00001
d_cycMax	0.368	5.568	0.137	0.140	0.804	1.022	0.00001
d_hystMax	0.437	4.392	0.248	0.200	1.167	0.807	-0.00002

APPENDIX 3 Description of the header of the final database flatfile

The final database flatfile includes, for each waveform (199 for three components) all the ground motion parameters described in Table 2, Table 3 and Table 4. The header is also complemented by the following information:

name: name of the file (excluding extension and component)

EVENT_NAME: event name as reported in the ESM database

EVENT_ID: event name as reported in the ESM database

EVENT_DATE_YYYYMMDD: event date

EVENT_TIME_HHMMSS: event time

EVENT_LATITUDE_DEGREE: event latitude

EVENT_LONGITUDE_DEGREE: event longitude

EVENT_DEPTH_KM: event depth

MAGNITUDE_W: event moment magnitude

MAGNITUDE_L: event local magnitude

NETWORK: recoding network

STATION_CODE: code of the recording station

STATION_NAME: name of the recording station

STATION_LATITUDE_DEGREE: station latitude

STATION_LONGITUDE_DEGREE: station longitude

STATION_ELEVATION_M: station elevation on the sea level

LOCATION: location of the sensor

SENSOR_DEPTH_M: depth of the sensor

VS30_M/S: Vs,30 of the site of the recording station

SITE_CLASSIFICATION_EC8: site classification according to EC8

MORPHOLOGIC_CLASSIFICATION: morphologic classification

EPICENTRAL_DISTANCE_KM: epicentral distance (km)

EqID: earthquake ID in the CPTI catalogue

EPICENTRAL_AREA: name of the epicentral area in the CPTI catalogue

PLACE_NAME SC: name of the place where the intensity was observed

LAT: latitude of the macro data point

LON: longitude of the macro data point

MCS: MCS intensity (if available)

EMS-98: EMS-98 intensity

COUNTRY: country

REFERENCE: reference for the macro data point



D_MDP_EPI: distance between the MDO and the event epicentre

D_MDP_ST: distance between the recording station and the MDP

APPENDIX 4 Characteristics of the modelled SDOF systems

Table 8: Masonry building typologies: defining parameters.

Building Typology	T [s]	Fy [g]	δy [m]	δu [m]
M1_L	0.211	0.168	0.0019	0.0089
M1_M	0.355	0.133	0.0042	0.0135
M1.w_L	0.211	0.178	0.0020	0.0094
M1.w_M	0.355	0.141	0.0044	0.0143
M1.v_L	0.211	0.132	0.0015	0.0070
M1.v_M	0.355	0.105	0.0033	0.0107
M2_L	0.268	0.146	0.0026	0.0104
M2.w_L	0.268	0.155	0.0028	0.0111
M2.v_L	0.268	0.116	0.0021	0.0082
M3_L	0.192	0.248	0.0023	0.0117
M3_M	0.322	0.196	0.0051	0.0176
M3_H	0.437	0.142	0.0067	0.0202
M3.w_L	0.192	0.263	0.0024	0.0124
M3.w_M	0.322	0.208	0.0054	0.0187
M3.w_H	0.437	0.151	0.0071	0.0214
M3.v_L	0.192	0.196	0.0018	0.0093
M3.v_M	0.322	0.155	0.0040	0.0140
M3.v_H	0.437	0.112	0.0053	0.0160
M3.sm_L	0.192	0.296	0.0027	0.0140
M3.sm_M	0.322	0.234	0.0060	0.0210
M3.sm_H	0.437	0.170	0.0080	0.0241
M4_L	0.173	0.358	0.0026	0.0149
M4_M	0.290	0.283	0.0059	0.0222
M4_H	0.393	0.223	0.0086	0.0260
M4.w_L	0.173	0.379	0.0028	0.0158
M4.w_M	0.290	0.300	0.0063	0.0235
M4.w_H	0.393	0.237	0.0091	0.0276
M4.v_L	0.173	0.283	0.0021	0.0118
M4.v_M	0.290	0.223	0.0047	0.0176
M4.v_H	0.393	0.177	0.0068	0.0206
M5_L	0.173	0.263	0.0019	0.0110
M5_M	0.290	0.208	0.0044	0.0164
M5_H	0.393	0.165	0.0063	0.0192
M5.w_L	0.201	0.279	0.0028	0.0140
M5.w_M	0.338	0.221	0.0063	0.0211
M5.w_H	0.459	0.152	0.0080	0.0239
M5.v_L	0.192	0.208	0.0019	0.0098
M5.v_M	0.322	0.165	0.0043	0.0148
M5.v_H	0.437	0.119	0.0057	0.0170

M5.sm_L	0.192	0.314	0.0029	0.0148
M5.sm_M	0.322	0.248	0.0064	0.0223
M5.sm_H	0.437	0.180	0.0085	0.0256
M6_L-PC	0.211	0.324	0.0036	0.0171
M6_M-PC	0.355	0.256	0.0080	0.0260
M6_H-PC	0.481	0.168	0.0097	0.0290
M6_L-MC	0.211	0.358	0.0040	0.0236
M6_M-MC	0.355	0.283	0.0088	0.0350
M6_H-MC	0.481	0.186	0.0107	0.0387
M7_L	0.153	0.508	0.0030	0.0233
M7_M	0.258	0.401	0.0066	0.0336
M7_H	0.350	0.317	0.0096	0.0386

Table 9: Non-designed reinforced concrete buildings: defining parameters

Building Typology	T [s]	Fy [g]	δy [m]	δu [m]
RC1_L	0.539	0.207	0.0150	0.0451
RC1_M	0.854	0.124	0.0224	0.0674
RC1_H	1.304	0.072	0.0304	0.0915
RC2_L	0.539	0.278	0.0201	0.0606
RC2_M	0.854	0.166	0.0300	0.0904
RC2_H	1.304	0.097	0.0407	0.1227
RC3_L	0.539	0.240	0.0174	0.0523
RC3_M	0.854	0.143	0.0259	0.0781
RC3_H	1.304	0.083	0.0352	0.1060

Table 10: DCL reinforced concrete buildings: defining parameters

Building Typology	T [s]	Fy [g]	δy [m]	δu [m]
L_RC1-III_L	0.437	0.227	0.0108	0.0324
L_RC1-III_M	0.642	0.164	0.0168	0.0504
L_RC1-III_H	0.913	0.115	0.0239	0.0717
L_RC1-II_L	0.437	0.363	0.0173	0.0518
L_RC1-II_M	0.642	0.263	0.0269	0.0806
L_RC1-II_H	0.913	0.185	0.0382	0.1147
L_RC1-I_L	0.437	0.502	0.0239	0.0716
L_RC1-I_M	0.642	0.363	0.0371	0.1114
L_RC1-I_H	0.913	0.255	0.0528	0.1584
L_RC2-III_L	0.437	0.305	0.0145	0.0434
L_RC2-III_M	0.642	0.220	0.0225	0.0676
L_RC2-III_H	0.913	0.155	0.0321	0.0962
L_RC2-II_L	0.437	0.487	0.0232	0.0695
L_RC2-II_M	0.642	0.352	0.0361	0.1081
L_RC2-II_H	0.913	0.248	0.0513	0.1538

L_RC2-I_L	0.437	0.673	0.0320	0.0960
L_RC2-I_M	0.642	0.487	0.0498	0.1494
L_RC2-I_H	0.913	0.342	0.0709	0.2125
L_RC3-III_L	0.437	0.263	0.0125	0.0375
L_RC3-III_M	0.642	0.190	0.0195	0.0584
L_RC3-III_H	0.913	0.134	0.0277	0.0830
L_RC3-II_L	0.437	0.421	0.0200	0.0600
L_RC3-II_M	0.642	0.304	0.0311	0.0934
L_RC3-II_H	0.913	0.214	0.0443	0.1328
L_RC3-I_L	0.437	0.581	0.0276	0.0829
L_RC3-I_M	0.642	0.420	0.0430	0.1290
L_RC3-I_H	0.913	0.295	0.0612	0.1835

Table 11: DCM reinforced concrete buildings: defining parameters

Building Typology	T [s]	Fy [g]	δy [m]	δu [m]
M_RC1-III_L	0.437	0.266	0.0127	0.0459
M_RC1-III_M	0.642	0.176	0.0180	0.0742
M_RC1-III_H	0.913	0.117	0.0242	0.0995
M_RC1-II_L	0.437	0.426	0.0203	0.0735
M_RC1-II_M	0.642	0.282	0.0288	0.1187
M_RC1-II_H	0.913	0.187	0.0387	0.1592
M_RC1-I_L	0.437	0.589	0.0280	0.1015
M_RC1-I_M	0.642	0.389	0.0398	0.1639
M_RC1-I_H	0.913	0.258	0.0534	0.2199
M_RC2-III_L	0.437	0.391	0.0186	0.0594
M_RC2-III_M	0.642	0.258	0.0264	0.0959
M_RC2-III_H	0.913	0.171	0.0355	0.1286
M_RC2-II_L	0.437	0.625	0.0297	0.0950
M_RC2-II_M	0.642	0.413	0.0423	0.1534
M_RC2-II_H	0.913	0.274	0.0568	0.2058
M_RC2-I_L	0.437	0.864	0.0411	0.1312
M_RC2-I_M	0.642	0.571	0.0584	0.2119
M_RC2-I_H	0.913	0.379	0.0784	0.2842
M_RC3-III_L	0.437	0.337	0.0160	0.0513
M_RC3-III_M	0.642	0.223	0.0228	0.0828
M_RC3-III_H	0.913	0.148	0.0306	0.1110
M_RC3-II_L	0.437	0.540	0.0257	0.0820
M_RC3-II_M	0.642	0.357	0.0365	0.1324
M_RC3-II_H	0.913	0.237	0.0490	0.1776
M_RC3-I_L	0.437	0.746	0.0355	0.1133
M_RC3-I_M	0.642	0.493	0.0505	0.1829
M_RC3-I_H	0.913	0.327	0.0677	0.2454

Table 12: DCH reinforced concrete buildings: defining parameters

Building Typology	T [s]	Fy [g]	δy [m]	δu [m]
H_RC1-III_L	0.437	0.251	0.0119	0.0557
H_RC1-III_M	0.642	0.141	0.0144	0.0814
H_RC1-III_H	0.913	0.093	0.0193	0.1092
H_RC1-II_L	0.437	0.401	0.0191	0.0890
H_RC1-II_M	0.642	0.225	0.0231	0.1302
H_RC1-II_H	0.913	0.149	0.0309	0.1747
H_RC1-I_L	0.437	0.554	0.0263	0.1230
H_RC1-I_M	0.642	0.311	0.0319	0.1799
H_RC1-I_H	0.913	0.206	0.0427	0.2413
H_RC2-III_L	0.437	0.368	0.0175	0.0719
H_RC2-III_M	0.642	0.207	0.0211	0.1052
H_RC2-III_H	0.913	0.137	0.0284	0.1411
H_RC2-II_L	0.437	0.588	0.0280	0.1151
H_RC2-II_M	0.642	0.331	0.0338	0.1683
H_RC2-II_H	0.913	0.219	0.0454	0.2258
H_RC2-I_L	0.437	0.813	0.0386	0.1590
H_RC2-I_M	0.642	0.457	0.0467	0.2325
H_RC2-I_H	0.913	0.303	0.0627	0.3119
H_RC3-III_L	0.437	0.317	0.0151	0.0621
H_RC3-III_M	0.642	0.178	0.0183	0.0908
H_RC3-III_H	0.913	0.118	0.0245	0.1218
H_RC3-II_L	0.437	0.508	0.0242	0.0994
H_RC3-II_M	0.642	0.286	0.0292	0.1453
H_RC3-II_H	0.913	0.189	0.0392	0.1949
H_RC3-I_L	0.437	0.702	0.0334	0.1373
H_RC3-I_M	0.642	0.394	0.0404	0.2008
H_RC3-I_H	0.913	0.261	0.0541	0.2693